

OPTIMIZATION OF SOLAR ENERGY HARVESTING: BUILDING  
INFRASTRUCTURE AND STATISTICAL OPTIMIZATION

By

Zaid I. Almusaied

A thesis submitted to the Graduate Council of  
Texas State University in partial fulfillment  
of the requirements for the degree of  
Master of Science in Technology  
with a Major in Industrial Technology  
May 2016

Committee Members:

Bahram Asiabanpour, Chair

Semih Aslan

Harold Stern

Farhad Ameri

**COPYRIGHT**

by

Zaid I. Almusaied

2016

## **FAIR USE AND AUTHOR'S PERMISSION STATEMENT**

### **Fair Use**

This work is protected by Copyright Laws of the United States (Public Law 94-553, section 107). Consistent with fair use as defined in the Copyright Laws, brief quotations from this material are allowed with proper acknowledgement. Use of this material for financial gain without the author's express written permission is not allowed.

### **Duplication Permission**

As the copyright holder of this work I, Zaid I. Almusaied, authorize duplication of this work, in whole or in part, for educational or scholar purpose only.

## **DEDICATION**

I dedicate this thesis to my mother, *Soad*, whose memory has continually inspired me to stay driven in the pursuit of my goals.

## ACKNOWLEDGEMENTS

I would like to express deepest gratitude to my advisor ***Dr. Bahram Asiabanpour*** for his full support, expert guidance, understanding and encouragement throughout my study and research. Without his incredible patience and timely counsel, my thesis work would have been a frustrating and overwhelming pursuit. I also express my appreciation to ***Dr. Semih Aslan***, ***Dr. Harold Stern***, and ***Dr. Farhad Ameri*** for having served on my committee. Their thoughtful questions and comments were valued greatly.

I would also like to thank ***Dr. Andy Batey***, ***Dr. Cassandra Hager*** and fellow Engineering Technology faculty for helping me with my coursework and academic research during my graduate years.

Finally, I would like to thank my father, ***Ibrahim Almusaied***, for his unconditional support during the last few years; I would not have been able to complete this program without his continuous encouragement.

## TABLE OF CONTENTS

	Page
ACKNOWLEDGEMENTS .....	v
LIST OF TABLES .....	viii
LIST OF FIGURES .....	ix
ABSTRACT .....	xiii
 CHAPTER	
I. INTRODUCTION .....	1
Background .....	1
The History of Photovoltaic (PV) .....	3
Semiconductors .....	4
Acceptors Impurities .....	6
Donors Impurities .....	8
The p-n Junction .....	9
The Photovoltaic Effect .....	10
Photovoltaic Materials .....	16
Solar Electric System and Photovoltaic Cells Efficiency .....	19
The Scope of the Research .....	21
II. SOME SOURCES OF INEFFICIENCY IN SOLAR PANELS .....	23
Power Conversion .....	23
Remedy .....	23
Solar Panel Orientation and Tilting .....	24
Remedy .....	25
Temperature .....	25
Remedy .....	28
Dust and Dirt .....	29
Remedy .....	32
Aging and Degradation .....	33
Remedy .....	34
Other Factors and Compounding Effects .....	34
III. ELECTRICAL COMPONENTS .....	36
Photovoltaic Panels .....	36
Loads .....	39

Calculating the Area of the PV Panel Using the Reported Efficiency .....	40
IV. THE WEB-BASED DATA ACQUISITION SYSTEM .....	41
Data Acquisition Network .....	41
The eGauge .....	42
The RS485 Converter .....	43
The Sunny Sensorbox .....	44
RS485 Power Injector .....	45
Ambient Temperature Sensor .....	46
The PV Panel Surface Temperature Sensor .....	46
DC Current Transducers .....	47
Router, Ethernet Cables, and Wires .....	48
V. MECHANICAL SYSTEM .....	49
Background and Implementation .....	49
VI. RESPONSE SURFACE METHODOLOGY .....	62
Introduction .....	62
Factors Identification .....	63
Factors Levels in Feasible Ranges .....	65
Design of Experiments .....	68
Conducting the Experiments .....	70
Data Analysis .....	72
Optimization .....	78
Investigation the Sun's Postion and Its Effect on the Optimum Point .....	80
Efficiency Calculations .....	82
Validation .....	84
VII. CONCLUSIONS AND FUTURE WORKS .....	85
Conclusions .....	85
Future Works .....	86
APPENDIX SECTION .....	88
REFERENCES .....	103

## LIST OF TABLES

Table	Page
1. Energy gap .....	12
2. Various influential parameters .....	35
3. The PV electrical specifications.....	37
4. Mechanical specifications .....	38
5. The specifications of the rheostat .....	39
6. Bill of materials.....	60
7. Parts list.....	61
8. The four uncoded factors with their three levels .....	67
9. The four coded factors with their three levels .....	67
10. The analysis of the data using Minitab .....	73
11. Minitab optimization results .....	79
12. Validation sample of data .....	84



## LIST OF FIGURES

Figure	Page
1. The energy of the sun.....	2
2. Pure silicon atoms with their covalent bonds .....	5
3. The difference in band gap for insulator, metal, and semiconductor.....	6
4. The creation of holes.....	7
5. The creation of free electrons .....	9
6. The p-n junction.....	10
7. Wavelength and energy.....	13
8. A photovoltaic device consisting of p-n junction .....	14
9. Equivalent electrical circuit .....	15
10. The efficiency record .....	18
11. Photovoltaic cell structures .....	19
12. The two I-V curves.....	26
13. Temperature effect on PV cell efficiency.....	27
14. Solar-intensity reduction in response to dust deposition .....	31
15. The PV panel used in the research.....	36
16. The IV diagrams .....	38
17. The rheostat used in the research.....	39
18. The wiring diagram of the system used in the research.....	41
19. The eGauge .....	43

20. The Chiyu BF-430 .....	44
21. The sunny sensor box.....	45
22. The power injector .....	45
23. The ambient temperature sensor used in this research.....	46
24. The temperature sensor .....	47
25. The DC current transducer .....	47
26. Square tube draft .....	51
27. Base plate draft .....	51
28. The caster draft .....	51
29. Fixed base plate.....	52
30. Square tube adaptor plate.....	52
31. Square tube column.....	52
32. Sweeping mechanism pin .....	53
33. D-plate draft .....	53
34. T-slot bar .....	53
35. The final assembly draft.....	54
36. Parts draft and list .....	54
37. Various parts draft and how to assemble .....	55
38. Water jet machine used in the production.....	55
39. 3D printer used in the production .....	56
40. Chop saw used in the production .....	56

41. SuperStruts .....	56
42. The rotating base plate used in the mechanical system .....	57
43. The square tube adaptor base used in the mechanical system .....	57
44. The square steel legs assembled to fixed base plate and caster .....	57
45. The T-slot plastic bolt adaptor used in the mechanical system .....	58
46. The D-plate with several tilt angle settings.....	58
47. The two D-plates attached to the PV panel holder structure .....	59
48. The final assembly of the mechanical system.....	59
49. General model of a process or system .....	64
50. The process diagram of the experiment .....	65
51. Minitab .....	68
52. Using Minitab to create Box-Bhenken design of RSM .....	69
53. Using Minitab GUI to select unblocked Box-Bhenken runs .....	69
54. Using Minitab GUI to identify the high and low levels for each factor .....	69
55. Using Minitab GUI to select the design specifications.....	70
56. The PV panel with levels of treatments .....	70
57. The PV panel subjected to the treatment during the experiment .....	71
58. Using the Minitab GUI to analyze the results.....	72
59. Four-in-one residual plot generated by Minitab .....	74
60. The main effect plot generated using Minitab for the yield response.....	75
61. The surface plot of the yield response as generated using Minitab .....	76

62. The interaction plot .....	76
63. Contour plot of the yield response .....	77
64. The optimization graph generated by Minitab .....	80
65. The main effect for the runs before mid-day .....	81
66. The main effect plot for the runs in the afternoon .....	82
67. The received irradiance for the two PV panels .....	83
68. The various recorded efficiency of the two PV panels during the experiment.....	84

## **ABSTRACT**

Renewable energy is the path for a sustainable future. The development in this field is progressing rapidly and solar energy is at the heart of this development. The performance and efficiency limitations are the main obstacles preventing solar energy from fulfilling its potential. This research intends to improve the performance of solar panels by identifying and optimizing the affecting factors. For this purpose, a mechanical system was developed to hold and control the tilt and orientation of the photovoltaic panel. A data acquisition system and electrical system were built to measure and store performance data of the photovoltaic panels. A design of experiments and response surface methodology were used to investigate the impact of these factors on the yield response as well as the output optimization. The findings of the experiment showed an optimum result with a tilt of  $60^\circ$  from the horizon, an azimuth angle of  $45^\circ$  from the south and a clean panel condition. The wind factor showed insignificant impact within the specified range. This work can be continued by investigations on the materials, geometry, cleaning and cooling systems, and involving some other environmental and physical factors.

# I. INTRODUCTION

## Background

The relation between man and the sun is ancient. The sun has played a massive role in the history of mankind. Some old civilizations even had spiritual belief in the power of the sun. According to Hsieh (1986), the sun is a giant nuclear reaction that transforms four million tons of hydrogen to helium per second. The earth will receive only a tiny amount of the sun generated energy (Hsieh, 1986). The radiated energy from the sun must be equal to the energy it produces to ensure its structural stability (Sorensen, 2011). The evidence of this stability over the last 3 billion years can be seen by the relative stability of the temperature of the earth's surface (Sorensen, 2011). Oxidized sediments and fossil remains reveal that the water fluid phase has been presented through this time (Sorensen, 2011). The earth's orbit around the sun is slightly elliptical, making the distance between the two vary throughout the year. The earth and sun are 91.4 million miles apart in January compared to 94.5 million miles in July; this leads to an annual disparity of 3%–4% in the irradiance at the edge of the atmosphere (Shepherd & Shepherd, 2014). Although the earth receives just a tiny fraction of the Sun's generated energy, it is still a massive amount of energy. The earth's radiation reception rate is  $1.73 \times 10^{17}$  J/s, and in a year made up of 365.25 days, the total amount of radiation is  $5.46 \times 10^{24}$  J (Shepherd & Shepherd, 2014). Boylestad and Nashelsky (1989) stated that the received energy at sea level is about 1 kW/m<sup>2</sup>. There are strong links of all known forms of energy resources to the sun and how they are used by mankind (Tester, Drake, Driscoll, Golay, and Peters, 2012; See Figure 1).

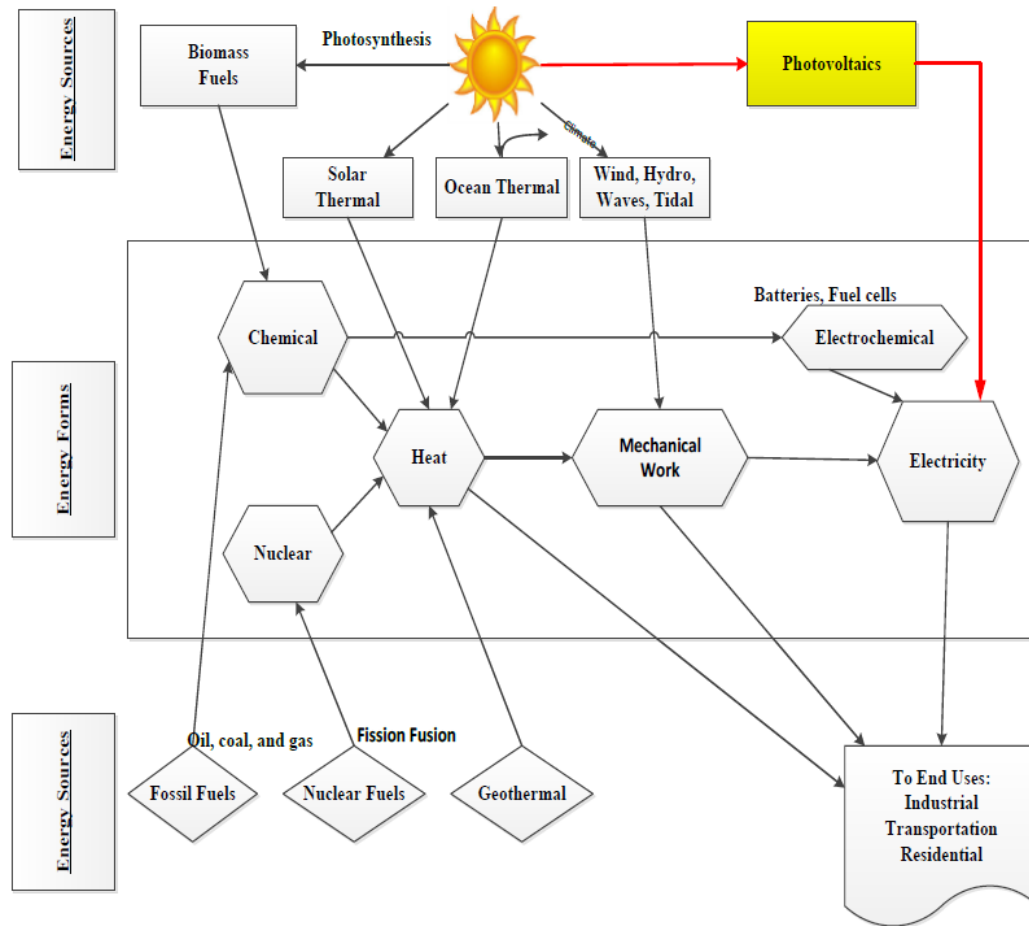


Figure 1. The energy of the sun. The figure shows the sun and its relation to various energy sources. Adapted from “Sustainable Energy: Choosing Among Options,” by J. W. Tester et al, 2012 p.12.

The fossil fuels used today were formed over the course of thousands of years, but they are consumed rapidly (Shepherd & Shepherd, 2014). In 2009, the world consumed 11,164.3 million tons of oil equivalent (Shepherd & Shepherd, 2014). Comparing this consumption with the amount of received solar radiation during the same year, one will find that the input of solar radiation was 11,300 times greater than the world’s total

primary energy consumption (Shepherd & Shepherd, 2014). This increase in consumption of the limited fossil fuel resources, the environmental concerns, plus the fluctuations in the oil market have led humanity to search for more clean and renewable sources of energy. For a long time, solar energy has been one of the most promising, sustainable energy sources. Generating electricity from the incident light has many challenges, and one of the greatest challenges is the drop in efficiency.

### **The History of Photovoltaic (PV)**

The word photovoltaic is composed of two parts. The first is photo, which comes from the Greek word  $\phi\omega\varsigma$  (*phōs*) meaning light, and the second is volt, which comes from the Italian scientist, Alessandro Volta, who invented the battery (electrochemical cell) (Smee, 1849). Volt is the unit measurement of the electromotive force. Using semiconductor materials to directly convert the solar energy into electricity is called photovoltaic (Prasad, 2011). This effect was first discovered in 1839 by the French physicist Edmund Becquerel in an electrolytic cell exposed to light (Prasad, 2011). In 1877, Adams and Day detected the effect in solid selenium (Bube, 1960) as cited by (Goswami, Kreith, & Kreider, 2000). The progress in this field continued in 1904 when Albert Einstein published a paper on the photoelectric effect (Prasad, 2011). This paper led to Einstein being awarded the Nobel Prize for physics and drew more attention to this field. (“The Nobel prize”, n.d.).

The competition between the United States of America and the Soviet Union to reach outer space during the Cold War helped to escalate the attention to this field as solar energy can be used to energize satellites, space stations, and vehicles to name a few. The research done by Bell Laboratories and RCA in 1954 achieved efficiency up to six



percent. They used devices made of p and n types of semiconductors (Bube, 1960) as cited by (Goswami, Kreith, & Kreider, 2000). The efficiency of solar panels has improved since then, but efficiency is still considered one of the biggest sources of limitation for the advancement of solar energy harvesting.

## **Semiconductors**

Semiconductors are materials with conductivity between insulators and conductors. Semiconductors such as silicon, germanium or gallium-arsenide will be insulators with a relatively narrow energy gap ( $0.1 \text{ eV} < E_g < 3 \text{ eV}$ ) at low temperatures and pure chemical condition (Kaltschmitt & Rau, 2007). Silicon and germanium lie in the fourth column of the periodic table. As the nucleus of the atom will contain the positively charged protons plus the uncharged neutrons, the negatively charged electrons will orbit around the nucleus. The electrons have four quantum numbers (shell, subshell, orbital, and spin). The quantum numbers describe the energy level, distance from the nucleus, angular momentum, orbitals, and spin. The electrons are fermions that will have discrete energy levels with no two electrons having the same four quantum number (Pauli Exclusion Principle). The electrons that are farthest from the nucleus are the highest in energy level. The valence layer (shell) is the outer layer. A silicon valence layer has four electrons. These electrons will form tight covalent bonds with the neighboring atom's valence electrons. Thus, a pure crystal of material will be formed. A high energy will be required to free an electron from the bond and make it a charge carrier. This makes the pure semiconductor materials act as an insulator with low conductivity at room temperature (Shepherd & Shepherd, 2014). Applying a voltage across such material at

room temperature will cause only a tiny amount of current (leakage current) to pass through (Kaltschmitt & Rau, 2007).

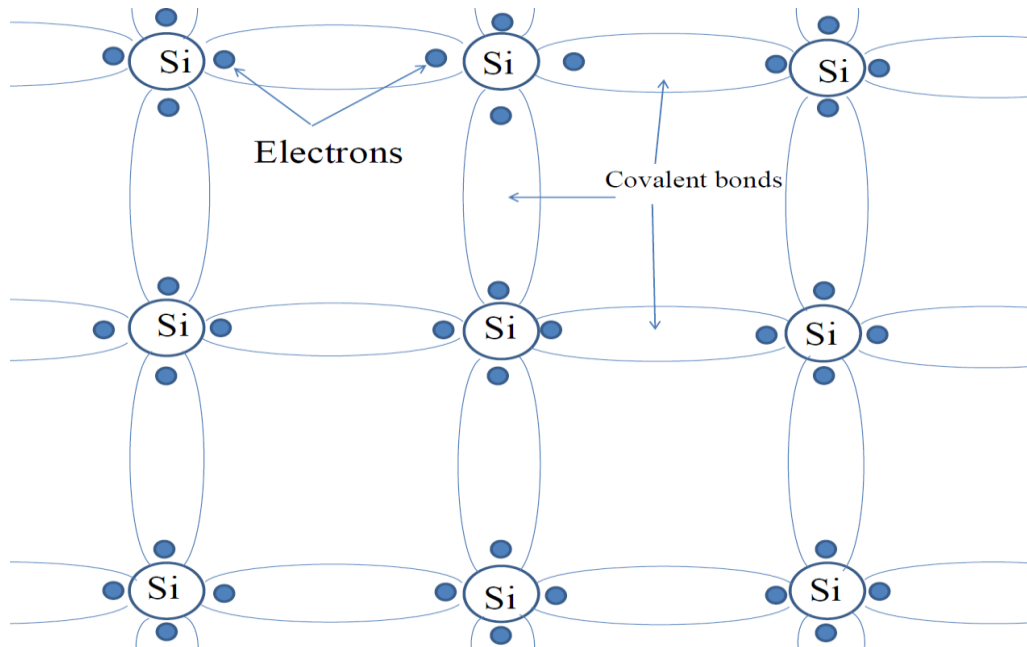


Figure 2. Pure silicon atoms with their covalent bonds. Adapted from “Electricity and Electronics a Survey,” (3<sup>rd</sup> ed.), by D. R. Patrick, & W. Stephen, 1996 p.246.

The electrons in the valence band, when energetic, will jump to a higher band. The higher band is called a conduction band where a small amount of impressed force would release the electrons from the atom. These electrons are responsible for the conduction of heat and electricity. The energy distinction between a valence electron and the inner subshell of the conduction band is called a band gap. Insulators have high band gaps ( $>3$  eV) (Goswami et al., 2000).

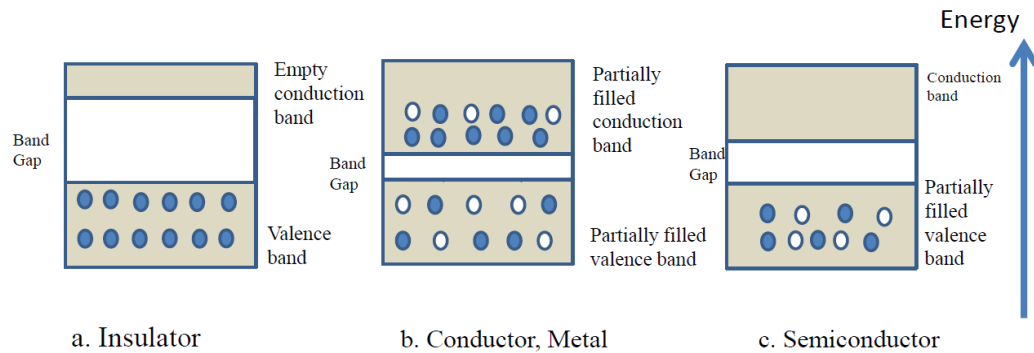


Figure 3. The difference in band gap for insulator, metal, and semiconductor. The insulator, a., with the bigger band gap and empty conduction band. The conductors, b. Metal, have a small band gap and sometimes there will be an overlap between the valence and conduction band. The conduction band is partly filled with electrons. The semiconductor, c., has a moderate band gap and has a partially filled valence band. Adapted from “Principle of Solar Energy,” by D. Y. Goswami, F. Kreith, and J. F. Kreider, 2000 p. 414.

To increase the conductivity of the pure semiconductors, impurities are added to them. Bell Telephone Laboratories in New Jersey, U.S.A., introduced this technology in the 1950s (Shepherd & Shepherd, 2014). We can categorize impurities into two groups:

#### Acceptors Impurities

Materials from the third column of the periodic table like boron, aluminum, gallium, and indium will be used to dope the pure semiconductor materials. These materials, the impurities, have three electrons in their outer shells. The acceptor impurities have their name because they can accept free electrons. The impurity atoms constitute three covalent bonds with their neighboring atoms using their three outer

electrons. This will lead to a hole forming at the fourth side, as the covalent bond with the adjacent pure semiconductor atoms will lack the necessary electron. Applying potential difference across the doped semiconductors will result in migration of holes. This kind of doping forms a p-type, positive, semiconductor. The holes are the majority of the charge carriers. The free electrons are the minority of the charge carriers (Shepherd & Shepherd, 2014).

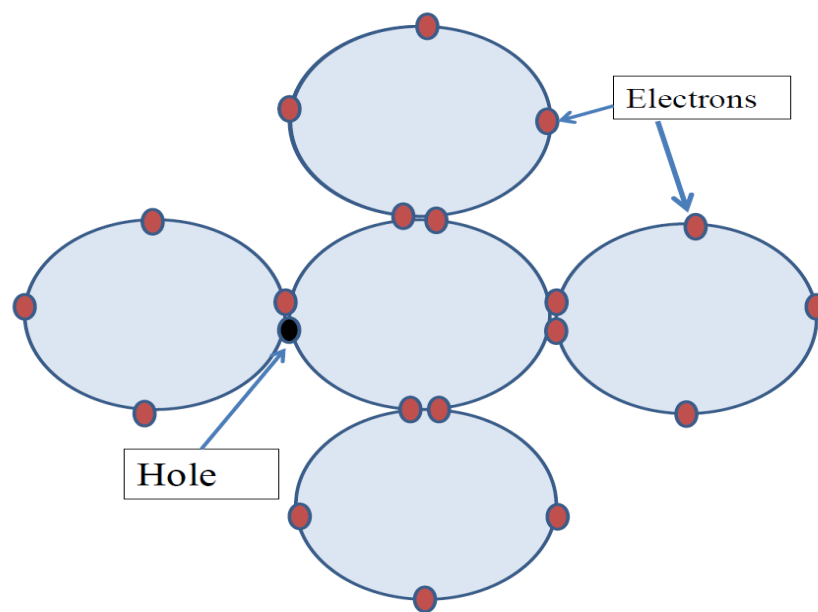


Figure 4. The creation of holes. The silicon atoms share their four valence electrons with their neighbors creating covalent bonds. When impurities from the third column of the periodic table are doped into the silicon they will create covalent bonds with the silicon atoms, but having only three electrons on their outer shell a hole will be created. Adapted from “Energy studies,” by W. Shepherd and D.W. Shepherd, 2014 p. 430.

### Donors Impurities

Materials from the fifth column of the periodic table, such as arsenic, phosphorus, and antimony, will be used to dope the pure semiconductors. These materials, the impurities, have five electrons in their outer shells. The impurity atom constitutes four covalent bonds with its neighboring atoms using its four outer electrons. This will leave the fifth electron of the impurity atom to lie in the valence shell. Such an electron can be easily freed from his original atom when applying electromotive force to the doped semiconductor. These impurities are called donors because they can supply free electrons. This kind of doping forms an n-type, negative, semiconductor. The free electrons are the majority of the charge carriers. The holes are the minority of the charge carriers (Shepherd & Shepherd, 2014).

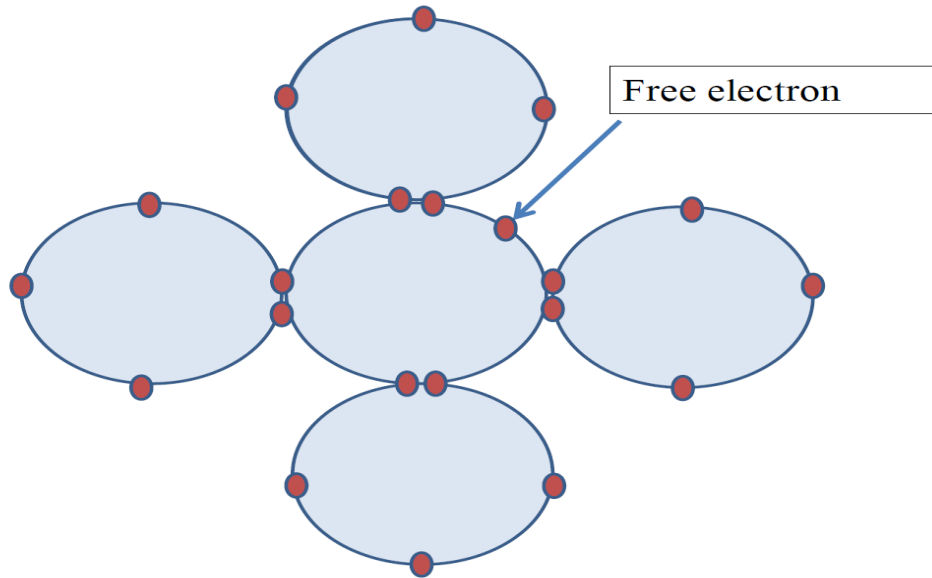


Figure 5. The creation of free electrons. The silicon atoms share their four valence electrons with their neighbors creating covalent bonds. When impurities from the fifth column of the periodic table are doped into the silicon they will create covalent bonds with the silicon atoms, but having five electrons on their outer shell free electrons will be excess. Adapted from “Energy studies,” by W. Shepherd and D.W. Shepherd, 2014 p. 430.

### **The p-n Junction**

The characteristic of the n-type materials will lead to an excessive amount of free electrons, while the p-type materials have, the opposite, holes. When contacting these two materials, the free electrons from the n-layer will jump to fill the holes in the p-layer. This situation will result in positive charges on the n-layer near the junction. The negative charges will be on the p-layer near the junction (Goswami et al., 2000). As a result of the carriers’ movement, an electrical field will be formed on the sides of the junction and thus a depletion area will be established (Kaltschmitt & Rau, 2007).

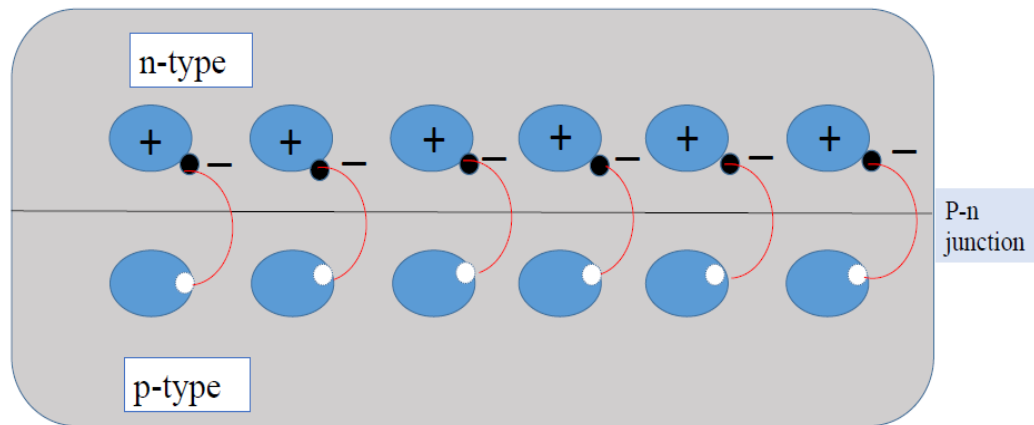


Figure 6. The p-n junction. The p-type material has an excess of holes while the n-type material has an excess of electrons. When they are attached together the electrons will move from the n-type toward the p-type while the holes will move from the p-type toward the n-type. The movements will continue until an electric field will be created due the accumulation of electrons on the p side of the junction and holes on the n side of the junction creating a depletion region. Adapted from “Principle of Solar Energy,” by D. Y. Goswami, F. Kreith, and J. F. Kreider, 2000 p. 415.

### **The Photovoltaic Effect**

According to Kaltschmitt and Rau (2007), as the light photon reaches the atom valence electron it will be absorbed by it. The absorption increases the electron’s energy. When the photon’s energy is equivalent or more than the energy band gap of the semiconductors, the electron will move to the conduction band. If the absorbed energy is less, the extra energy will transform into kinetic energy. Also, if the absorbed photon is more than what is needed to cross the energy band gap, as one photon can free only one

electron, the extra energy will also convert into kinetic energy. In both cases, the kinetic energy will manifest itself as heat (Kaltschmitt & Rau, 2007). This phenomenon is a major player in the conversion efficiency of photovoltaic devices.

The photon is a quantum of energy, as defined by Max Planck, and can be calculated by his equation

$$E_p = h\nu$$

Where  $h$  is Planck's constant ( $6.625 \times 10^{-34}$  J.sec), ( $\nu$ ) is the frequency. The frequency can be represented by its associated wavelength ( $\lambda$ ) and light speed ( $c$ ) by using the equation:

$$c = \nu\lambda$$

$$\nu = \frac{c}{\lambda}$$

$$E_p = \frac{hc}{\lambda}$$

From the above equation and for silicon, which has a band gap of 1.11 eV, we can calculate the wavelength of light that is capable of forming an electron-hole pair. This wavelength is 1.12  $\mu\text{m}$  or less (Goswami et al., 2000).



Table 1. Energy gap. Various energy gaps for materials that can be used for photovoltaic cells. Adapted from “Principles of Solar Engineering,” by D. Y. Goswami, F. Kreith, and J. F. Kreider, 2000, p. 417.

Material	Band gap (eV)	Material	Band gap (eV)
Si	1.11	CuInTe <sub>2</sub>	0.90
SiC	2.60	InP	1.27
CdAs <sub>2</sub>	1.00	In <sub>2</sub> Te <sub>3</sub>	1.20
CdTe	1.44	In <sub>2</sub> O <sub>3</sub>	2.80
CdSe	1.74	Zn <sub>3</sub> P <sub>2</sub>	1.60
CdS	2.42	ZnTe	2.20
CdSnO <sub>4</sub>	2.90	ZnSe	2.60
GaAs	1.40	AlP	2.43
GaP	2.24	AlSb	1.63
Cu <sub>2</sub> S	1.80	As <sub>2</sub> Se <sub>3</sub>	1.60
CuO	2.00	Sb <sub>2</sub> Se <sub>3</sub>	1.20
Cu <sub>2</sub> Se	1.40	Ge	0.67
CuInS <sub>2</sub>	1.50	Se	1.60
CuInSe <sub>2</sub>	1.01		

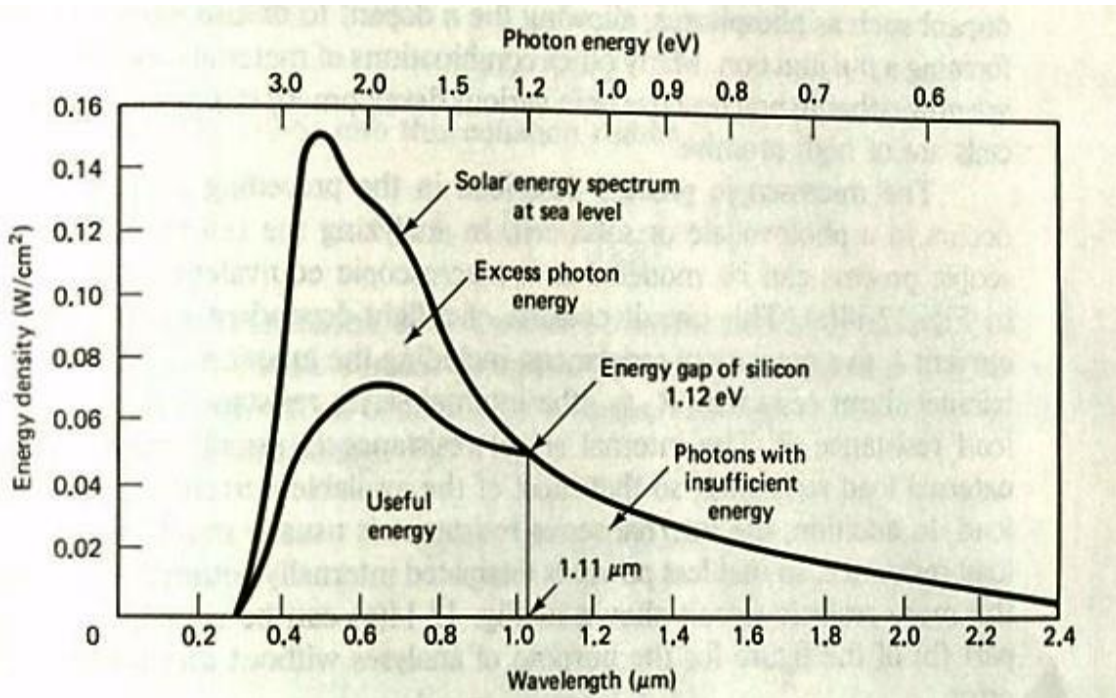


Figure 7. Wavelength and energy. The silicon photovoltaic cell uses only the photons that have certain wavelengths that will result on an energy equal to or above the silicon band gap. Adapted from “Solar Energy Engineering,” by S. Hsieh, 1986, p. 375.

The solar cell has a thin layer of n-type semiconductor, around  $0.2 \mu m$ , attached to a thicker layer of p-type semiconductor, around  $300 \mu m$  (Hsieh, 1986). The photovoltaic effect will result in the uses of the freed electrons through the connection terminals that connect the solar cell with the outer external resistance load to drive these freed electrons outside the p-n junction before they unite with the holes (Goswami et al., 2000).

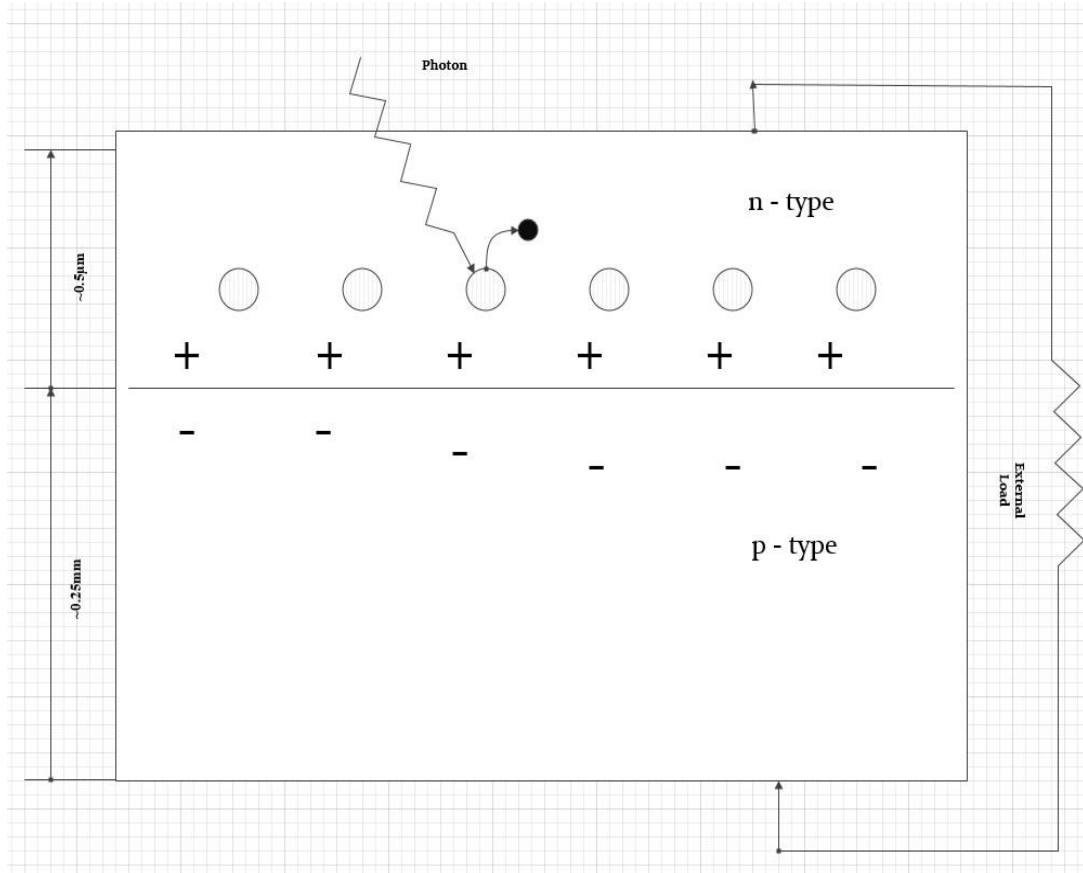


Figure 8. A photovoltaic device consisting of p-n junction. The photovoltaic effect happens when the solar radiation reaches a semiconductor and causes the separation of the positive and negative charge carriers. When connectors contact the photovoltaic device those carriers are driven out to external loads before recombination happens. Adapted from “Principle of Solar Energy,” by D. Y. Goswami, F. Kreith, and J. F. Kreider, 2000, p. 416.

The photovoltaic cell has an electrical equivalent of a current source, diode with  $R_{shunt}$ , and  $R_{series}$ .

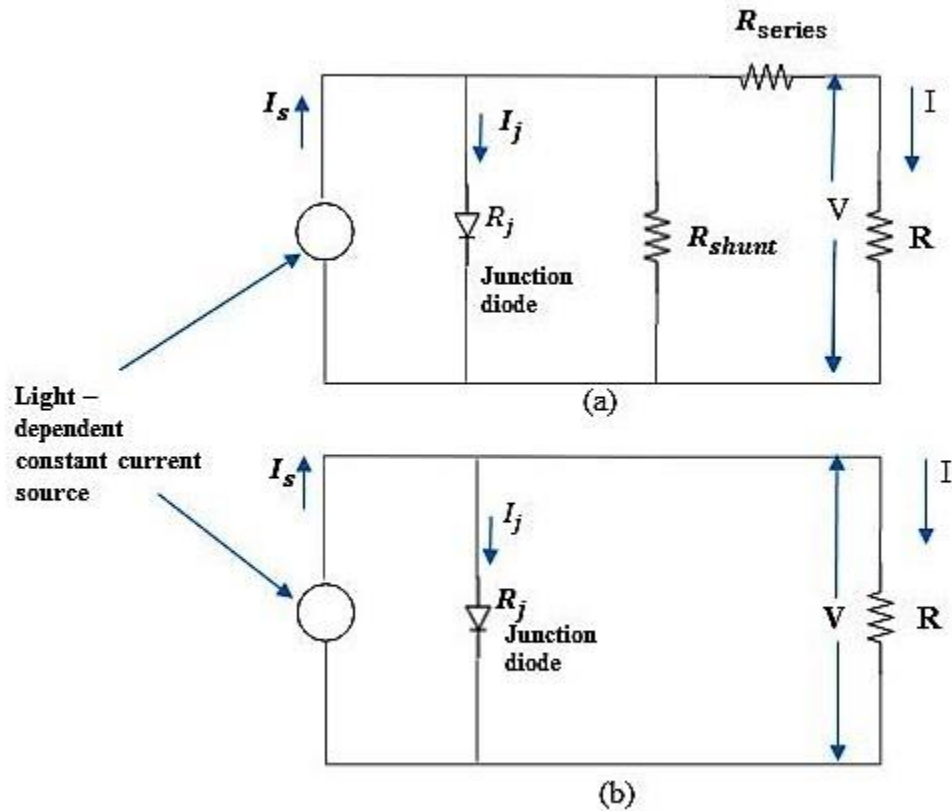


Figure 9. Equivalent electrical circuit. The photovoltaic cell can be replaced with an equivalent electrical circuit, (a), of a current source, diode, internal parallel shunt resistance, and internal series resistance. The internal shunt resistance is usually very much higher than the external load so that the load will have most of the current, while the series resistance is much less than the external load to ensure the minimum dissipating of energy in it. More practical drawing of the equivalent circuit, (b), will be without the shunt and series internal resistance. Adapted from “Solar Energy Engineering,” by S. Hsieh, 1986, p. 376.

Where:  $R_{series}$  is the internal resistance,  $R_{shunt}$  is the internal parallel shunt resistance,  $R_j$  is Junction resistance,  $I_s$  is the light dependent current from the equivalent current source,  $I_j$  is the junction current,  $T$  is the absolute temperature in kelvin, and  $K$  is Boltzmann's constant

$$I_j = I_o \left[ \exp \left( \frac{eV}{KT} \right) - 1 \right]$$

$I_o$  is the saturation current, also known as leakage or diffusion current.

$$I = I_s - I_j$$

$$I = I_s - I_o \left[ \exp \left( \frac{eV}{KT} \right) - 1 \right]$$

### **Photovoltaic Materials**

The most common photovoltaic modules, or panels, in the market are based on silicon. These photovoltaic panels vary in the way the silicon is manufactured (Prasad, 2011). Amorphous silicon cells are formed using uncrystallized silicon. No expensive production techniques are required (Shepherd & Shepherd, 2014). They are often named as thin silicon film, and this thin layer will be placed on various surfaces, such as glass. The color will be usually dark matte (Prasad, 2011). The efficiency for this kind of photovoltaic cell is low (typically 5-8%) (Prasad, 2011). Monocrystalline solar cells are thin wafer. The wafer is cut from a large single crystal; thus it is expensive and uses a lot of silicon (Shepherd, 1975). The cells are bluish-black in color (Prasad, 2011). According to Menzies (1998) as cited by (Prasad, 2011), the efficiency is the best for such cells for a given module area and the cells will have a long life when well manufactured.

Polycrystalline solar cells came as development in the manufacturing process. Prasad (2011) stated that the cells are thin wafers cut from multiple crystal silicon. They are distinguished by their blue color, but they could be another color. These cells are the most common panels on the market. Two-thirds of the installed photovoltaic cells used crystalline silicon in 2009, but the use of thin film technologies is steadily increasing EIA (2010) as cited in (Tester et al., 2012). Choosing between polycrystalline and monocrystalline is a tradeoff between cost and efficiency (Tester et al., 2012).

Many materials other than silicon have been investigated to determine their cost and efficiency (Tester et al., 2012). Photovoltaic cells made of 1-3 $\mu$ m layers copper indium diselenide (CuInSe<sub>2</sub> or CIS), with thin over layers of silica (SiO<sub>2</sub>) and cadmium zinc sulfide (CdZnS) or cadmium sulfide (CdS) all have higher efficiency than silicon based photovoltaic devices with similar manufacturing cost (Tester et al., 2012). CIS cells have serious sustainability and toxicity problems. For example, the protection of the workers, the environmental impact of the mining for elements like Zn, In, Mo, Se, Cd, and Cu, and the end-of-life disposal should be considered during the manufacturing process. This can also affect the regional supply and demand for these materials and raise the cost (Tester et al., 2012).

Cadmium telluride (CdTe) is also a very promising material to use. It has an energy band gap of 1.5 eV. This will make it very suitable for the solar spectrum. This material has the same issues and concerns as the CIS; it may harm the environment, the workers, and lead to resource depletion. Nevertheless, it is very promising especially with improvement in manufacturing technology and reducing the cost with better efficiency (Tester et al., 2012).

## Best Research-Cell Efficiencies

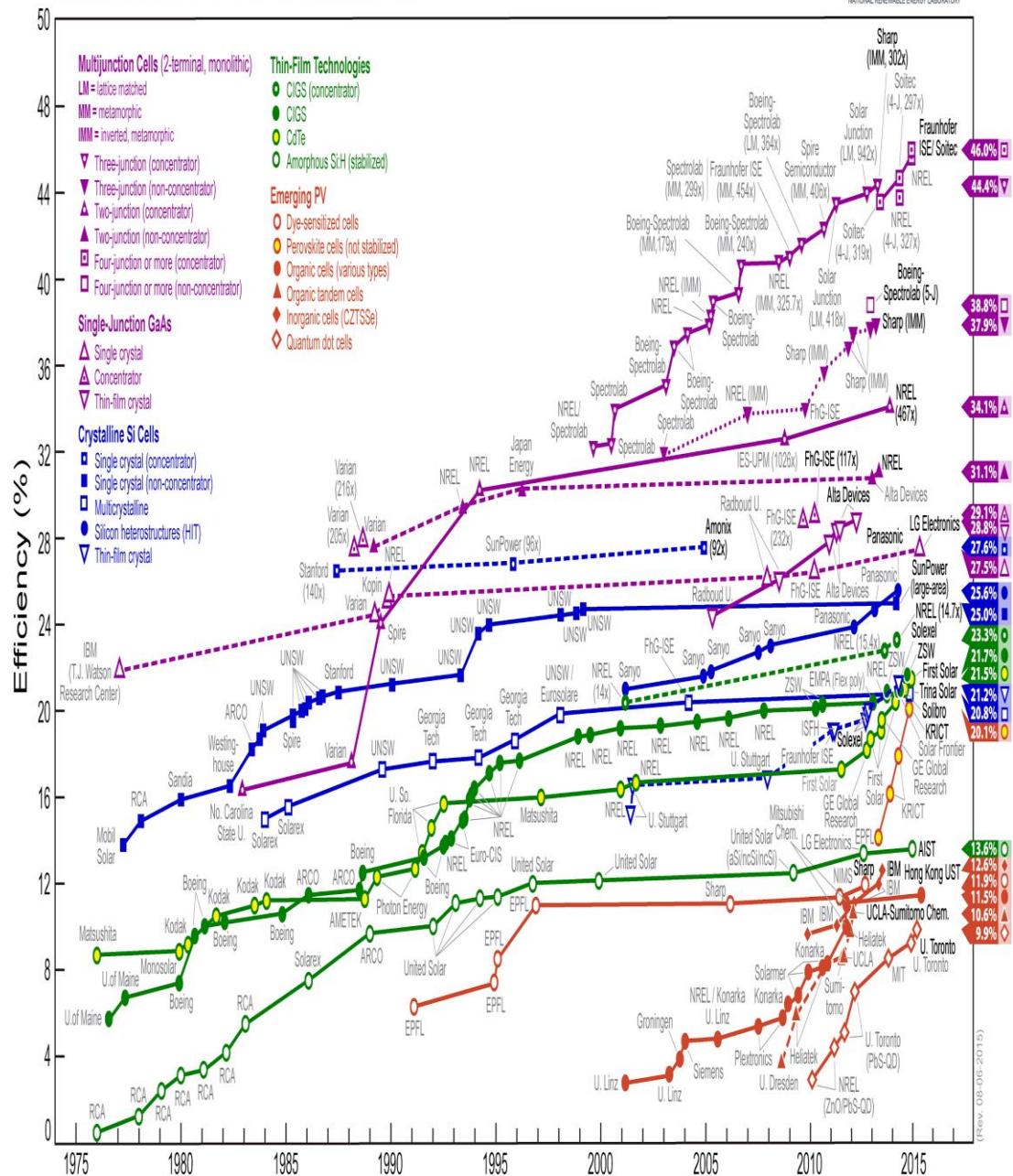


Figure 10. The efficiency record. The efficiency of different materials with different technologies as it improves and reported every year. Adapted from “Efficiency Chart” by National Renewable Energy Laboratory,” 2015.

## Solar Electric System and Photovoltaic Cells Efficiency

Shepherd and Shepherd (2014) stated that photovoltaic cell structures can be formed by connecting cells together to constitute a module, and modules are connected to establish an array

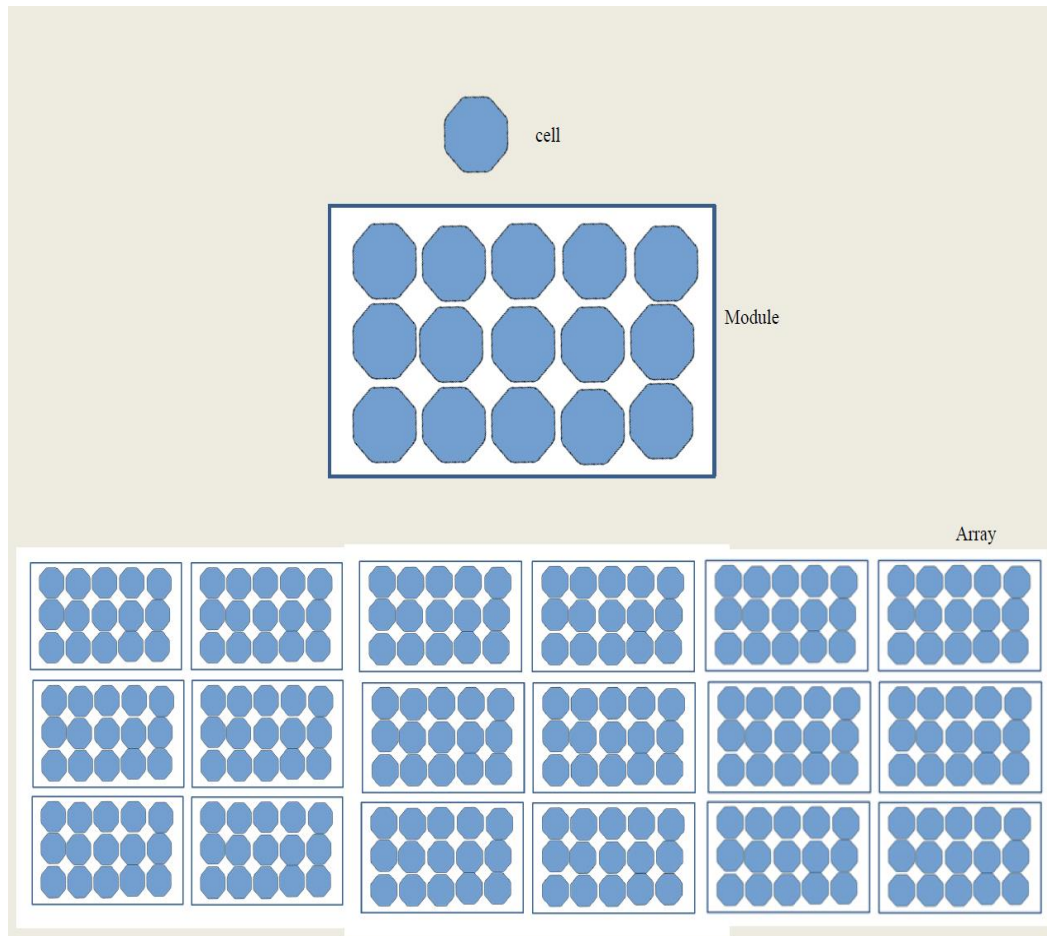


Figure 11. Photovoltaic cell structures. Cells connected together to form a module, and modules connected together to form an array. Adapted from “*Energy studies*,” by W. Shepherd and D.W. Shepherd, 1975 p. 428.



ˆ Solar electric systems can be categorized into three group according to Chiras (2011): grid-connected, grid-connected with battery backup, and off-grid (Chiras, 2011).

The performance of solar cells and modules can be calculated through their efficiency.

The efficiency and some of the causes of losses stated by Prasad (2011) include

- Losses due to the collecting metallic grid that covers the surface of the photovoltaic cell; this grid is responsible of collecting the electrons that the photovoltaic effect will produce.
- Losses due to reflection; some of the sun's radiation will be reflected from the surface of the cell.
- Losses due to the combination of the freed electrons by the photovoltaic with the holes in the semiconductors.
- Losses due to insufficient energy absorbed by the electrons to cross the energy band gap. On the other hand, if the photon absorbed by the electron is more than the required energy, the extra energy will be converted to heat.
- Losses due to shading of the photovoltaic cell, a drop in voltage will occur when part of the cell or the module is shaded.

By reviewing some of the sources of losses we can conclude these sources are inherent in the materials used to manufacture the cells or modules. The solar electrical system components also will be a source of losses. These components are power connections, inverters, control and interconnection equipment, and batteries (Tester et al., 2012).

## **The Scope of the Research**

The future of the solar energy depends on improving both the efficiency and performance of the PV panels. The performance and efficiency of the PV panels depend on many factors such as:

- The manufacturing and material specifications where the maximum theoretical efficiency is limited
- Improving the power conversion for the PV panels systems, where the conversion from the generated DC to AC causes losses in efficiency
- Environmental factors (e.g. temperature, wind )
- Status of the PV panels (e.g. orientation, tilting)

In this research the focus is on the environmental factors and status of the PV panels where the designated location and time/date play a significant role on the performance of the PV panels. The purposes of the research are to identify the significant factors, their range, and the optimum settings to improve the performance of the PV panel. The controllable factors include tilt, orientation (azimuth), wind, and the level of cleanness.

Suitable infrastructure to conduct this research has been developed. The infrastructure includes a mechanical system, an electrical system, and a web-based data acquisition system. The experiment was designed and analyzed using response surface methodology and design of experiments.

The first limitation for this research includes the limited number of PV panels with the proper infrastructure to conduct the runs in the same time. Instead, a single panel

was utilized for all runs. This way, sun irradiance varies during the experiment, although the use of the secondary solar panel in the flat position and clean status as the control sample (not subject to treatment) and difference between power generations in two panels eliminated the irradiance variability. Other limitations include uncontrollable factors associated with the temperature and general weather conditions. Date, time, and designated location can be considered as the delimitations. The study focuses on the aforementioned controllable factors and their three levels of treatment.

## **II. SOME SOURCES OF INEFFICIENCY IN SOLAR PANELS**

In this chapter, the sources of inefficiency in solar panels and the available remedies are discussed.

### **Power Conversion**

Photovoltaic (PV) panels produce a direct current (DC) as result of the photovoltaic effect. The direct current needs to be converted into an alternating current (AC) in order to connect to a utility grid or home appliances. Some systems use central inverters for all panels in one location while other systems have a single inverter for each PV panel. The process of converting direct current electricity into alternating current electricity causes losses in efficiency. Many commercial inverters are available with various levels of efficiency; some are up to 96%–98% while others might be less than 95% efficient. Inverters are significantly less efficient when used at the low end of their maximum power. Many inverters are most efficient in the 30%–90% power range (Central Electricity Regulatory Commission., 2011).

### **Remedy**

Micro-inverters have several advantages, according to their producers. In addition to having alternating current directly from each PV panel, a 5%-25% increase in power output is typical for micro-inverters when compared to traditional PV panels utilizing central inverters (GreenRay, Inc., 2010). Furthermore, micro-inverter manufacturers claim that by having inverters decentralized, the system will be easier to install and maintain with 40% fewer components. The micro-inverter seems promising, but as Daniel Sullivan states (2012), the concept of having an electronic device exposed to weather conditions may affect its performance and reliability.

There have been many attempts to directly obtain alternating current electricity from solar panels. These attempts were found in different U.S. patents. Although they succeeded in getting the alternating current directly from the PV panels, they couldn't achieve practical, reliable, or even an equal-in-efficiency system performance compared to the use of inverters. This can be seen in the following patents (U.S. Patent No. **4,075,034**, 1978), (U.S. Patent No. 4,577,052, 1986), (U.S. Patent No. 4,728,878, 1988), (U.S. Patent No. 6,774,299, 2004), (U.S. Patent No. 2005/0034750, 2005), (U.S. Patent No. 2010/0139735, 2010), (U.S. Patent No. 8,492,929 B2, 2013).

### **Solar Panel Orientation and Tilting**

The orientation of the panel has an impact on its performance. The angle and direction of the tilt is important to receive the incident insolation and generate electricity from the PV panels. At the same time, orientation has another impact on the accumulation of dust and dirt on the panel's surface. The geographic location plays a great role in determining the orientation. Common belief states that the PV panel's appropriate tilt angle should be the same as the latitude of the PV panel location on earth (Mondol, Yohanis & Norton, 2007). It should be tilted (if the PV panel location is above the equator) southward and toward the sun. Yet, some places have diverse weather conditions with winters that are cloudier than summer, or the average morning and afternoon insolation is not identical (Mondol et al., 2007). The result will be more energy received by the PV panels when the azimuth angle is either east or west of due south (for locations above the equator) (Mondol et al., 2007).

## Remedy

To maximize the received incident insolation, it is best to have a tracking system that will follow the sun to obtain the best result with perpendicular solar radiation flux on the surface of the PV panel. Many commercial tracking systems are available. These systems are either single or dual axis trackers (Neitzel, 2016). Having a sun tracker will provide a better output but is also more expensive. Fixed PV panels with the appropriate tilt for a specific location (optimum tilt angle is site dependent) can produce quality energy (Mondol et al., 2007). Another aspect to consider is the season. To maximize the incident insolation on the surface during summer, an inclination of  $10^{\circ}$ – $15^{\circ}$  less than the latitude is usually required compared to  $10^{\circ}$ – $15^{\circ}$  more during winter (Duffie & Beckman, 1991) as cited by (Mondol et al., 2007).

## **Temperature**

The efficiency of PV panels will be affected by the operating temperature. The standard operating temperature for PV panels is  $25^{\circ}$  C with  $1000 \text{ W/m}^2$  of solar flux (Al-Sabounchi, 1998). PV panels, like all other semiconductor devices, are sensitive to temperature. The gain in temperature decreases the band gap, and that will decrease the open circuit voltage ( $V_{oc}$ ). The maximum power is provided by the following equation:

$$P_m = V_m I_m = (FF) V_{oc} I_{sc} \quad (1)$$

The fill factor (FF in Equation 1) will also decrease substantially with the increase in temperature. The short-circuit current will increase slightly (ZONDAG, 2007) as cited by (Skoplaki & Palyvos, 2009).

$$\eta_c = \eta_{Tref} [1 - \beta_{ref}(T_c - T_{ref}) + \gamma \log_{10} GT] \quad (2)$$

Equation 2 defines the crystalline silicon efficiency where  $\eta_{Tref}$  is the module's electrical efficiency at the reference temperature,  $T_{ref}$ , and at solar radiation flux of 1000 W/m<sup>2</sup>. The temperature coefficient,  $\beta_{ref}$ , and the solar radiation coefficient,  $\gamma$ , are mainly material properties, having values of about 0.004 K<sup>-1</sup> and 0.12, respectively, for crystalline silicon modules. The temperature coefficient ( $\beta_{ref}$ ) is usually supplied by the manufacturer, along with  $\eta_{Tref}$ . The solar radiation coefficient  $\gamma$  is usually set to zero and then Equation (2) is reduced to Equation (3) (Skoplaki & Palyvos, 2009).

$$\eta_c = \eta_{Tref} [1 - \beta_{ref}(T_c - T_{ref})] \quad (3)$$

Figures 12 and 13 show the effect of temperature on voltage outputs and on the cell efficiency, respectively. It is clear from Figure 12 that the voltage output is higher at colder temperatures. Figure 13 shows that the PV cell efficiency is decreased as the temperature is increased over the standard operating temperature of 25° C.

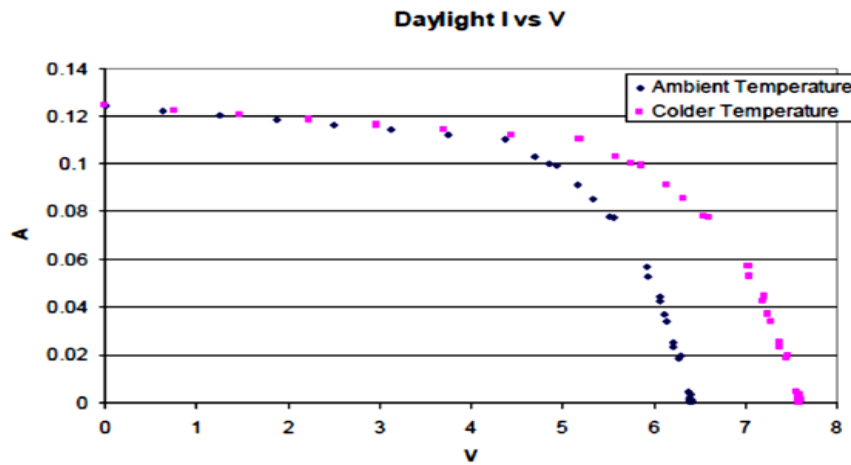


Figure 12. The two I-V curves. The I-V curves show the temperature dependence of the voltage output for a PV panel. The voltage output is greater at the colder temperature, adapted from “Photovoltaic Efficiency Lesson 2 the Temperature Effect,” by (Surles et al., 2009).

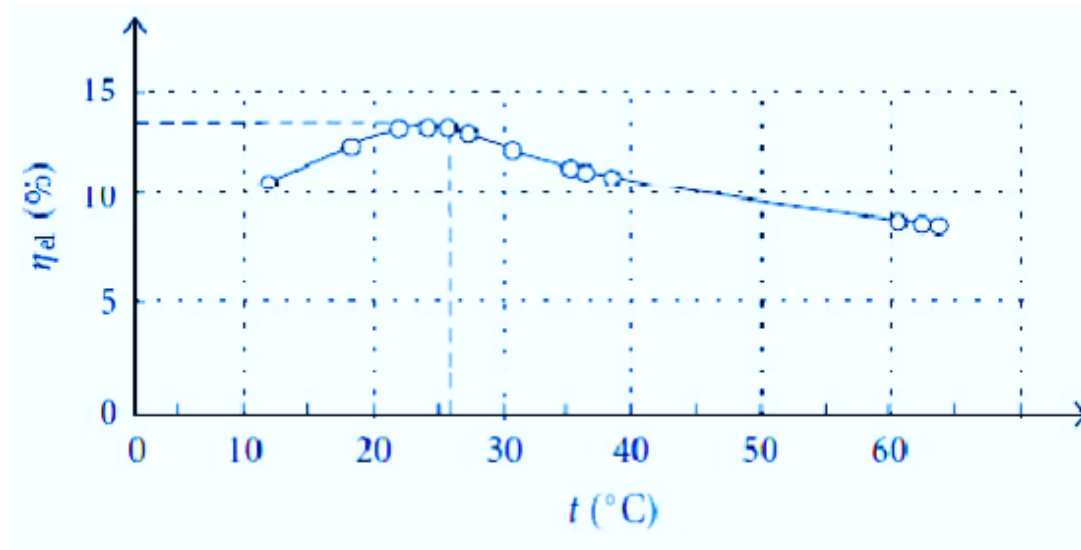


Figure 13. Temperature effect on PV cell efficiency. Adapted from “Improving the Power Generation from Solar PV Panel Combined with Solar Thermal System for Indian Climatic Condition.” By (Jaiganesh & Duraiswamy, 2013)

In addition to the ambient temperature and the PV panel materials, many other factors can affect the temperature of the cells. For instance, the wind velocity will impact the temperature. Higher air velocity will cause a drop in temperature resulting in better efficiency (Mekhilef, Saidur & Kamalisarvestani, 2012). Also covering the surface of the PV panel will increase the temperature, the increment can be 10° C from the normal temperature of the panel without any deposits (Dorobantu, Popescu, Popescu, & Craciunescu, 2011).



## Remedy

Cooling the PV panels to reduce cell temperature can be achieved actively or passively. An active cooling system requires an external power source to run the system, while a passive cooling system does not. Passive cooling can be achieved by installing PV panels on the roof with a space between them, which allows a natural air circulation behind the panels to reduce some of the heat. Another method to reduce the heat is painting the surrounding roof surface a white color. An active cooling system might use fans to force air circulation, or a water cooling system that pumps water on the PV panels' surface for a cleaning and cooling effect (Surles et al., 2009). When the heat collected from the PV panels' surface (either from the forced circulated air, water, or both) is used, the system is considered a hybrid photovoltaic thermal (PVT) system. Rear air ducting can cut down the operating temperature by 25° C (Brinkworth, Cross, Marshal, & Hongxing, 1997) as cited by (Odeh & Behnia, 2003). Increasing the rear gap will increase the cooling as a result of natural convection (Martin, Seitz, & Saman, 2003) as cited by (Odeh & Behnia, 2003). Additionally, a different technique with an additional glass surface above the PV panels provides more improvement with an air gap for more air circulation (Odeh & Behnia, 2003). Jaiganesh and Duraiswamy (2003) introduced a different method to generate more power by 1.12% and collect an additional 44.37% of heat from circulated water. They replaced the conventional five layers of the PV panels (G2T) from glass, EVA, PV cell, EVA, and Tedlar into G2G, with the last layer replaced by glass instead of Tedlar. All of the previously mentioned remedies not only help to improve the efficiency (by reducing the cell temperature), but they also increment the incident radiation resulting from the radiation refraction by water (when water is used as

a coolant), clean the surface, and reduce the risk of damaging the cells due to excessive heating (Odeh & Behnia, 2003).

### **Dust and Dirt**

Dust can be defined as fine, dry powder consisting of tiny particles of earth or waste matter on the ground, or carried in the air. These particles are less than 500 $\mu$ m in diameter (Mekhilef et al., 2012; Google Translate, N.D). The scattering of these tiny particles depend on their nature and the surrounding environment (Mani & Pillai, 2010). Many studies have been done to analyze and quantify the efficiency losses due to the dust accumulation (soiling) on the surface of PV panels. These various studies have been done with different methodologies, and they counted multiple factors that directly affect the density of accumulated dust on the panels' surfaces. Some studies were conducted in a laboratory environment with talcum, dust, sand, and cement particles to cover the PV panels, while other elements were introduced with moss (Sulaiman, Singh, Mokhtar, & Mohammed, 2014). In the experiment by Sulaiman et al. (2014), a light radiation of 310 W/m<sup>2</sup> was used on PV panels covered with talcum, sand, and moss. The output power was reduced by 9% to 31% when the talcum was placed on the panel surface; when the dust was used, the output dropped between 70% and 80%; and the moss impact resulted in a reduction between 77% and 83%. These experiments were conducted in an equatorial climate condition. Salim, Huraib, and Eugenio (1988) as cited by (Sulaiman et al., 2014) conducted a study near Riyadh (Saudi Arabia) on the performance of a PV system when the dust accumulated for a long term. The result after eight months was a reduction of 32% compared to an identical PV system tilted at 24.68° which was cleaned daily. Wakim did a similar study in Kuwait City and found the reduction was 17% after six

days and that the impact was higher during summer and spring than in fall and winter (Wakim, 1981) as cited by (Sulaiman et al., 2014). A study by Hassan, Rahoma, Elminir, & Fthy (2005) as cited by (Mani & Pillai, 2010) conducted in Egypt saw a drop between 33.5%–65% in the period of one to six months of exposure, respectively. Another study performed by Rajput and Sudhakar (2013) to quantify the impact of dust in central India with the latitude and longitude of 23° 25 N and 77° 42 E, and the time between 9:00 and 18:00. The dust reduced the power production by 92.11% and efficiency by 89%. Google conducted a study on the effects of dirt on PV panels at their headquarters in California, comparing two sets of PV panels. One was flat in carports, and the other was tilted on the roof. While the flat panel accumulated dirt on its top, rain washed away most dirt on the tilted panels, leaving some on the corners. After 15 months, Google crews cleaned the panels, which resulted in the doubling of energy output for the flat panels. The tilted panels did not show any significant difference. The Google crew waited another eight months and cleaned the PV panels again; the flat panels showed 36% improvement in efficiency (Lam, 2009). Grag (1973), as cited by Sulaiman et al. (2014), conducted an experiment in Roorkee, India. He found that the accumulated dust on a glass plate tilted at 45° would reduce the transmittance by an average of 8% when exposed for 10 days. Another study was done by Sayigh (1978), as cited by Sulaiman et al. (2014), to quantify the amount of dust per area, per day in Kuwait between April and June. Further studies conducted by Sayigh, Al-jandal, and Ahmed (1985), as cited by Sulaiman et al. (2014), on the effect of the accumulated dust on a tilted glass plate showed a reduction in plate-transmittance ranging from 64% to 17% for a tilt angle between 0° to 60° after 38 days. They also observed a reduction of 30% in the output gain after three days of dust

accumulation for the horizontal collector. A study was conducted by El-Shobokshy and Hussien (1993), as cited by Mani and Pillai (2010), in which they used different materials as dust (limestone, cement, and carbon particles). They also used halogen lamps as a constant source of light for the PV panels. They found that the finer particles have a greater impact than the coarser particles on the PV panels' performance for the same dust type.

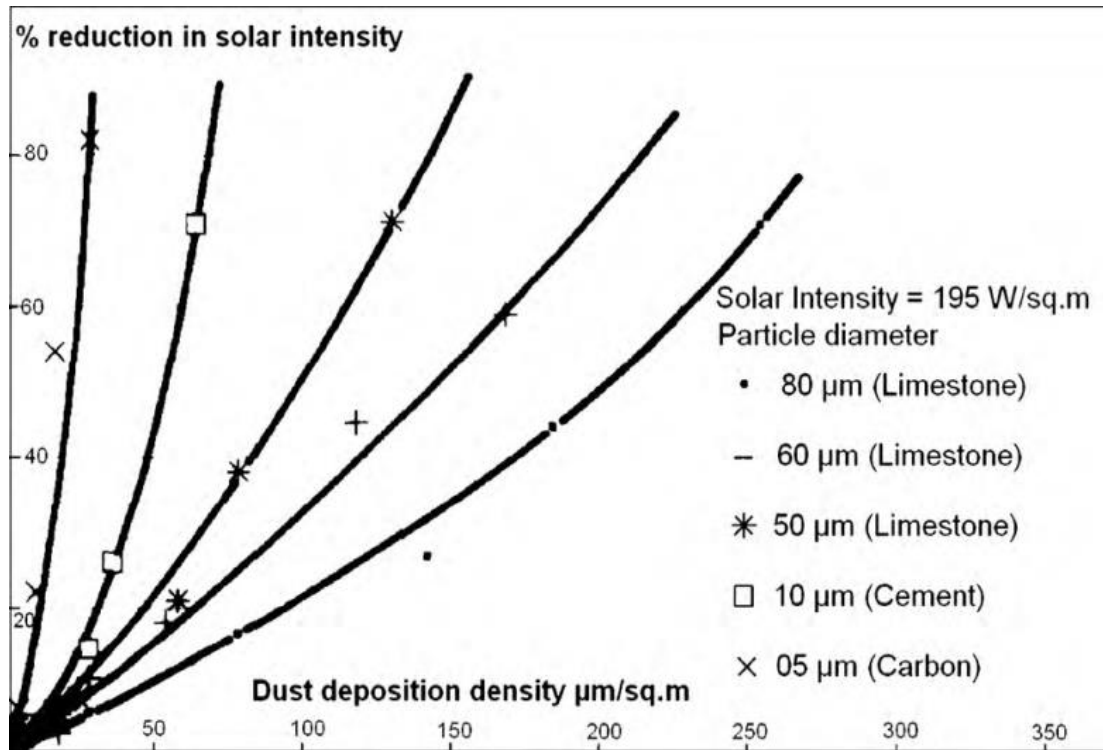


Figure 14. Solar-intensity reduction in response to dust deposition. Adapted from “Impact of Dust on Solar Photovoltaic (PV) Performance: Research Status, Challenges and Recommendations” by M. Mani and R. Pillai, 2010.

A study was done by Dorobantu et al., (2011) to illustrate the impact of the impurities left on the surfaces of the PV panels. The impurities included bird excrement,

pollution, and dust from traffic or agricultural activities. In addition to the drop in efficiency, the study detailed the damages that occur to the PV panels as the partial shading will increase the heat on the panel surface. The experiment was conducted using a thermal-vision camera and simulation software, in addition to the polycrystalline PV panels. Another study by Zorrilla-Casanova et al., (2011) found that the mean of daily energy losses throughout a year caused by dust accumulation on the surface of the PV panels is around 4.4%, while in long intervals without rain, losses can be higher than 20%. Adding to that, the irradiance losses were not constant during the day and were highly dependent on the angle of the incident light and the ratio between diffused and direct radiation. A study by Cano (2011) was done to extrapolate from the relationship between tilt angle and soiling by understanding its impact on the short-circuit current of the PV panel, which is directly proportional to the irradiance reaching the solar cells. The study, conducted in Arizona from January 2011 to March 2011, found that for an angle of  $0^\circ$ , the loss was 2.02% due to soiling. Meanwhile, an angle of  $23^\circ$  and  $33^\circ$  also showed some insolation losses but less than the  $0^\circ$ , with 1.05% and 0.96%, respectively, in three months.

### Remedy

Due to the significant impact of dust accumulation and soiling on the efficiency of PV panels, many methods have been developed and used to overcome this challenge. Some of the methods use passive, self-cleaning treatment, while others are active cleaning. Manual cleaning using water might not be practical as it carries a high cost, is time consuming, and requires an excessive use of water (Mazmumder et al., 2011). Among other possible cleaning methods, the natural removal of dust, such as wind, rain,

and gravity could be relied on to clean PV panels. There are also mechanical ways to remove of dust, such as brushing, blowing, vibration, and ultrasonic driving (He, Zhou, & Li, 2010). Passive cleaning can be done using a modification of the PV panel surface to make it non-sticky with less adhesion to the dust particles. This will be accomplished through a nano-film that covers the surface and is made of super-hydrophilicity material or super-hydrophobic material (Mazmumder et al., 2011; He et al., 2010). Another method is using a transparent electrostatics screen (EDS). The EDS has rows of transparent parallel electrodes embedded within a transparent dielectric film. To remove the dust particles, phased-voltage activates the electrodes and particles on the surface are charged with electrostatic. The particles are removed by a traveling wave generated by the applied field. More than 90% of the accumulated dust is removed within two minutes, and the energy used for this process is a very small fraction of the PV panel produced energy (Mazmumder et al., 2011). In addition to the previously mentioned methods, Moharram, Abd-Elhady, Kandil, and Elsherif (2013) used a water system that included a mixture of surfactants (anionic and cationic) to remove dust, which showed a constant efficiency.

### **Aging and Degradation**

The lifespan of the PV panels according to some manufacturers is 20 years (Honsberg & Bowden, N.D.). The efficiency of the panels will decrease with time, and an accurate quantification of power drop over time is known as the degradation rate. The median value of the degradation rate, in general, is 0.5% per year (Jordan & Kurtz, 2013). Many factors can contribute and cause this degradation. The environment (pollution is one major issue); discoloration of the encapsulation (EVA layer) or glass due to the

ambient temperature; lamination defects; mechanical stress; and humidity cell contact breakdown (Kaplan, 2012; Livingonsolarpower, 2013, June 10). The different technologies used to manufacture PV panels can cause different types of degradation. Crystalline modules will suffer irreversible light-induced degradation due to defects activated by the initial light exposure (Livingonsolarpower, 2013, June 10). Amorphous silicon cells may face a decrease in output power of 10%-30% in the first six months of light exposure, then it will stabilize (Livingonsolarpower, 2013, June 10).

### Remedy

To address this problem, better quality materials need to be used in solar panels, better manufacturing processes, improved packaging and assembly of the cells into module, and improved inspection, cleaning, and maintenance have been proposed (Livingonsolarpower, 2013, June 10).

### **Other Factors and Compounding Effects**

In addition to individual factors affecting solar panels' efficiency, there are other factors such as humidity and wind velocity. There is also a compounding of different factors that may affect efficiency as well. Mekhilef et al., (2012) studied and summarized these effects, described in the following table.

Table 2. Various influential parameters. A brief summary of different influential parameters on the PV cell performance adapted from “Effect of Dust, Humidity and Air Velocity on Efficiency of Photovoltaic Cells.” By (Mekhilef et al., 2012)

<b>Factor</b>	<b>Dust</b>	<b>Humidity</b>	<b>Air velocity</b>	<b>Efficiency</b>
<b>Dust</b>	More dust settlement	Insignificant effect	Insignificant effect	Drops
<b>Humidity</b>	Causes more dust coagulation	-	Insignificant effect	Mostly drops Surges occasionally
<b>Air velocity</b>	More dust deposition Less dust deposition	Decreases	-	Improves



### III. ELECTRICAL COMPONENTS

#### Photovoltaic Panels

The photovoltaic (PV) panels used in this research are manufactured by Eoply New Energy Technology Co., Ltd. They are Epolly 125M/72, 190 watt monocrystalline solar modules that contain 72 cells connected in series with the following dimensions: 125 X 125mm. The vendor claims high efficiency plus high transmission rate with low iron tempered glass, anti-aging EVA, high flame resistant back sheet, and anodized aluminum alloy (Solar Systems USA, Inc., 2012). This module should have a good durability and resistance to weather conditions like hail and wind (Solar Systems USA, Inc., 2012). The power generated by these PV panels should be 90% for ten years and 85% for twenty-five years. The PV panels passed a pressure test of 10000 Pa. They should also perform very well with low light (Solar Systems USA, Inc., 2012).



Figure 15. The PV panel used in the research. The model is Epolly 125M/72,92 190 watt monocrystalline with 72 cells.

Table 3. The PV electrical specifications. Electrical specification of the PV panels used in the research. Adapted from (Solar Systems USA, Inc., 2012).

open circuit voltage	44.9 V
optimum operation voltage ( $V_{mp}$ )	37.08 V
short circuit current ( $I_{sc}$ )	5.55 A
optimum operating current ( $I_{mp}$ )	5.15 A
maximum power at standard conditions ( $P_{max}$ )	190 W
cell efficiency	17.04 %
operating temperature	-40°C to 85°C
Maximum system voltage	1000 V
Pressure resistance	227g steel ball falls down from 1m higher under 60 m/s wind

Table 4. Mechanical specifications. Mechanical characteristics of the PV panels used in the research. Adapted from (Solar Systems USA, Inc., 2012).

solar cell	monocrystalline silicon solar cell 125x125 (mm)
number of cells	72 (6x12)
dimensions	1580x808x35mm (62.2x31.81x1.38)
weight	15 Kg (33.07 lbs)
front glass	3.2 mm (0.13inches) tempered glass
frame	anodized aluminum alloy

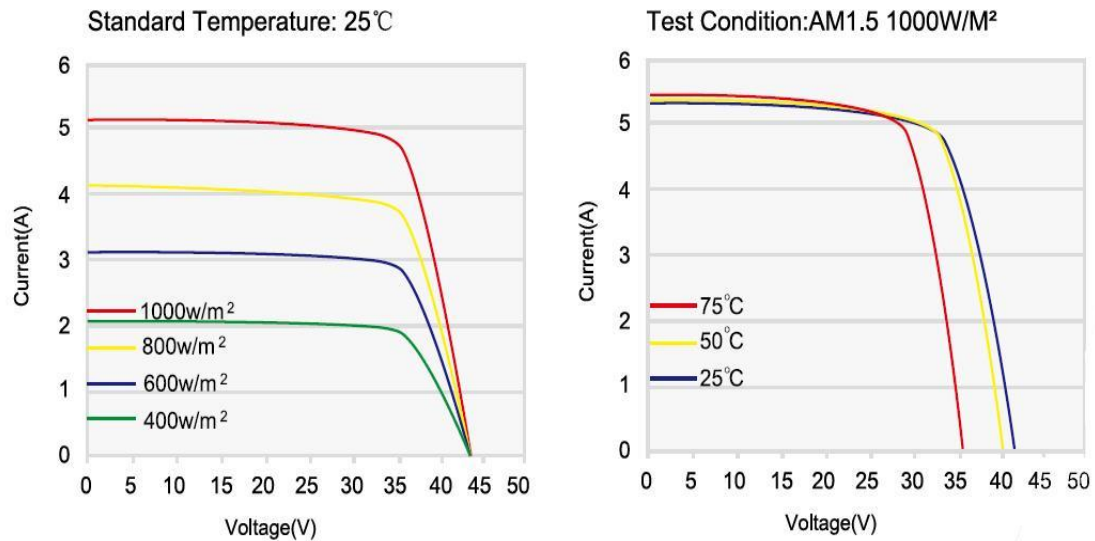


Figure 16. The IV diagrams. The IV diagrams for the PV panels used in the research with different irradiance and different temperature. Adapted from (Solar Systems USA, Inc., 2012).

## Loads

The loads used in this research are wire-wound, adjustable, tube resistors. These rheostats have the following specification as provided by the vendor:

Table 5. The specifications of the rheostat. Adapted from (Aliexpress.com, 2016).

weight	574g
rated power	300W
length	348 mm/13.7"
resistance	10 $\Omega$
main materials	metal, ceramic
installing hole size	6 mm/0.24"

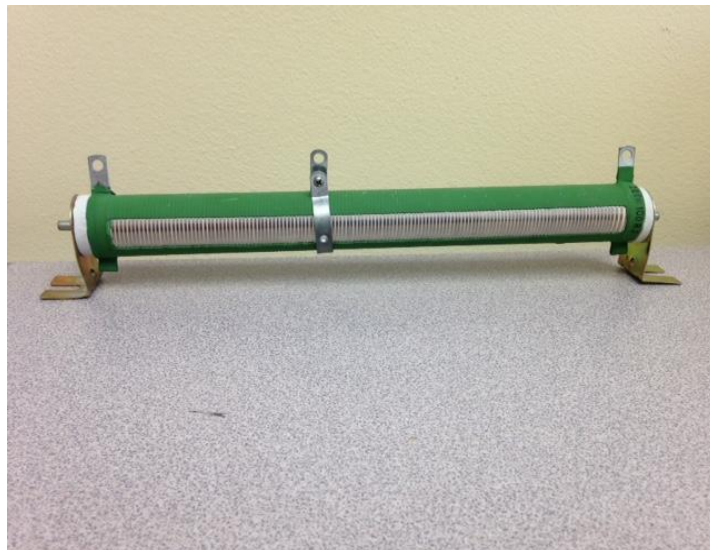


Figure 17. The rheostat used in the research. It has capability to dissipate 300W and it is 10  $\Omega$ .

The rheostats are used to dissipate the generated power. The PV panels' max power is 190 watts, Vmax is 37.08 v, and Imax is 5.15 amp. By Ohm's Law,  $R=V/I$

$$R_{\max} = \frac{37.08}{5.15}$$

$R_{\max}=7.2 \Omega$  as this resistance will achieve the max power with irradiance of  $1000 W/m^2$  and  $25^{\circ}C$ .\*

### **Calculating the Area of the PV Panel Using the Reported Efficiency**

The reported efficiency by the vendor is equal to 17.04% under the standard conditions where the irradiance is 1000 watts per square meter. The efficiency, the max power, and the standard conditions irradiance can be used to calculate the exact area of the usable solar cells in the PV panel.

$$\eta = \frac{(P_{out} \div A)}{(P_{in} \div A)}$$

Where P is the power and A is the area of the PV panel.

$$17.04\% = (190 \div A) \div (1000)$$

$$0.1704 \times 1000 = 190 \div A$$

$$A = 190 \div 170.4$$

$$A = 1.11502347 m^2.$$

## IV. THE WEB-BASED DATA ACQUISITION SYSTEM

### Data Acquisition Network

The data acquisition system used in this research consists of the eGauge, DC current transducer, power injector, RS485 to Ethernet converter, sunny sensor box, ambient temperature sensor, the PV panel temperature sensor, router, Ethernet cable, and wires.

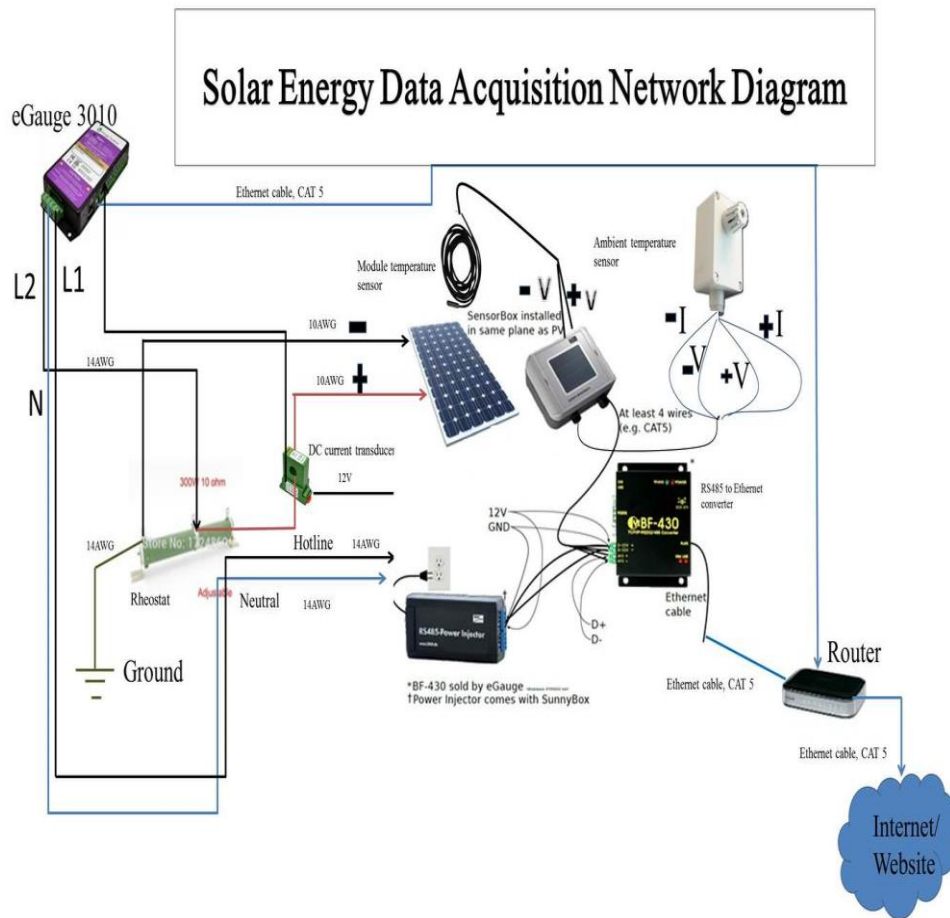


Figure 18. The wiring diagram of the system used in the research.

## **The eGauge**

The eGauge serves as an energy meter, data logger, and web server. It is the main unit in the data acquisition system used in this research. The eGauge model is EG 3010 and it is a product of eGauge system LLC. The eGauge measurement category is CAT III which can function in the building installation (eGauge Systems LLC, 2013). It can be connected to different types of electrical systems like single phase, split phase, and three phase (eGauge Systems LLC, 2013). There are three voltage connections in the device plus a 12 point connection for the current transducers which enable the eGauge to measure 12 individual circuits (eGauge Systems LLC, 2013). The eGauge has an Ethernet connection port on the side which enables it to communicate with other devices on an Ethernet TCP/IP network. The power, its variables, and data received from the sensors are stored in registers (eGauge Systems LLC, 2013). The eGauge has two options for the database that consists of either 16 or 64 registers, with more registers the storage duration will be less. The 16 and 64 registers can store data at one second granularity for 10 minutes in the volatile memory of the eGauge. For an average of one minute of data, the 16 and 64 registers can store data for one year (eGauge Systems LLC, 2013). The 16 registers can store the data for 29 years with average data of 15 minutes, while the 64 can only store for six years with average of one hour. The eGauge used in this research used 16 registers as this will give a longer time interval for storage plus the limited number of variables being followed (eGauge Systems LLC, 2013). The eGauge stores the collected data from multiple sensors that use the proper communication protocol. Modbus remote terminal unit (RTU) format is required for all external devices to be connected to the

eGauge with RS485 standard serial communication (eGauge Systems LLC, 2013). The eGauge will perform the communication with the external sensors via RS485 converter. The operation temperature of the eGauge can vary from -30 °C to 70 °C, max humidity 80% with 31 °C, pollution degree of 2 , and it can be used indoor or outdoor (eGauge Systems LLC, 2013). The eGauge can either set with a static internet protocol address (IP), or to obtain an IP automatically through a Dynamic Host Configuration Protocol (DHCP) server. The eGauge can export the recorded data as a CSV file; this feature is used to have the various collected data analyzed statistically during the research (eGauge Systems LLC, 2013). The wiring of this device is shown in figure 18.



Figure 19. The eGauge. It is an energy meter, logger and server used in this research.

### The RS485 Converter

The device used to perform the RS485 converter function is the Chiyu BF-430. Beside the RS485, this device also has the capability to convert RS232 to TCP/IP. The device is powered by 9 to 30 DC volts either from the standard plug in on the right side or through the power terminal on the left side. The device will take the input as serial



communication of RS485 through two wires on its side and convert it to Ethernet communication on the other side through an RJ 45 connection. The Ethernet side will connect to the router to create a local area network (LAN). The device has a web server where many configurations can be set. The configurations are baud rate, data bits, stop bits, and parity check (eGauge Systems LLC, 2015). The device is set either with static IP or as DHCP client. In this research, the device was set as DHCP client. The wiring of this device is shown in figure 18.



Figure 20. The Chiyu BF-430. It is a converter used to support the communication between the sunny sensor box and the eGauge feasible.

### **The Sunny Sensorbox**

This device is used for the measurement of the flux radiant solar energy per unit of area. The sunny sensor box also has connections with both the temperature ambient sensor and temperature PV panel probe. The sensors' data will be communicated via the RS485 power injector and the Chiyu BF-430 to the LAN and then the internet through the router. The device is crucial for the data system acquisition to collect the weather readings. The device operation temperatures vary from -27 °C to 70 °C (SMA America, LLC, 2011). The wiring of this device is shown in figure 18.



Figure 21. The sunny sensor box. It is used to measure the irradiance and communicate the temperature sensors signals to the eGauge via the Chiyu BF-430.

### **RS485 Power Injector**

The RS485 Power injector works by merging and integrating the sunny sensor box into the RS485 communication bus plus providing the sunny sensorbox with power to operate. The RS485 power injector can supply up to five sunny sensor boxes (SMA America, LLC, 2011). The wiring of this device is shown in figure 18.



Figure 22. The power injector. It is used in this research. The device supplies the sunny sensor box with power.

### **Ambient Temperature Sensor**

The ambient temperature is measured by TEMPSENSOR-AMBIENT which is a sensor composed of a PT100 measuring resistor enclosed by plastic cage (SMA America, LLC, 2011). The sensor will convey the data to the sunny sensor box then to the system. This sensor can measure from -30 °C to 80 °C (SMA America, LLC, 2011). The wiring of this device is shown in figure 18.



Figure 23. The ambient temperature sensor used in this research.

### **The PV Panel Surface Temperature Sensor**

The temperature of the PV panel is measured using the PT100-NR. This sensor is attached to the back of the panel to measure its temperature. The sensor is connected to the sunny sensor box where the temperature is then sent to the system. The temperatures that the sensor is capable of measuring vary from -20 °C to 110 °C (SMA solar technology AG, 2009). The sensor is composed of a PT100 measurement resistor inside plastic insulator. The wiring of this device is shown in figure 18.



Figure 24. The temperature sensor. It is used in this research to measure the PV panel temperature. The sensor is attached to the back of the panel.

### **DC Current Transducers**

These devices are used to measure the current generated by the PV panels. The model used in this research is CR5220-20-12V. The positive wire coming from the PV panel will go through the sensor to the load. The sensor will convey the equivalent of the direct current to the eGauge via connections on the side of the sensor. The input range varies from 0 to 20 amps. The DC current transducer is fed by 12 v DC (CRmagnetics Inc., n.d.). The wiring of this device is shown in figure 18.



Figure 25. The DC current transducer. It was used in this research to measure the current generated by the PV panels.

### **Router, Ethernet Cables, and Wires.**

A router is connected to the system to link the multiple devices and the internet providing a gateway. The router is set up as DHCP server to provide private IP addresses to the LAN components. The IPs started from 192.168.0.100 to 192.168.0.199 with network mask of 255.255.255.0. The router provides default gateway for the LAN which is 192.168.0.1 with network mask of 255.255.255.0.

The wires used to connect the system were 10 American gauge wire (AWG) and 14 AWG. These gauges can bear the current coming from the panel. The Ethernet cable used in this research is category five enhanced (CAT5E) which can carry information faster with less interference between the lines than CAT5. The connectors used on the Ethernet cable were registered jack 45 (RJ45) which has eight pins. The CAT5E Ethernet cable attached to the RJ45 with the same order of colored lines to the pins on both sides of the CAT5E cable forming the straight-through standard.

## **V. MECHANICAL SYSTEM**

### **Background and Implementation**

The mechanical system used in this research is a multi-task system. These tasks include holding, securing, changing the tilt, and changing the direction of the PV panel. The tilt and direction changing can be considered as a dual axis movement. The design and implementation of this system was assigned by Dr. Asiabanpour to a group of students as part of a tools design class. The group of students was comprised of Nicholas Hawkes, Trevor Scott, Sean Syring, and Simona Curry. The product development process (PDP) was used to design and implement this mechanical system. The System Modeling and Renewable Technology (SMART) lab was considered as the customer for the students. A rough implementation of the PDP steps was used, the steps included product planning, concept development, system-level design, detail design, testing and refinement, and production ramp-up (Ulrich & Eppinger, 2012). The key goals of the mechanical system product are to help to conduct the experiment, to make it user friendly, to produce it in the manufacturing lab, and to make multiple copies for other users. The customer needs were identified and used to establish the mechanical system specification, generate concepts and select concepts. The needs included the capability of the system to hold and secure the PV panel, capable of rotating the PV panel, capable of changing the tilt angle of the PV panel, ease of manufacture, ease of assembly, user friendly, meet the target budget, and withstand fast wind. The previous needs were also categorized into constraints (demands) and wishes. The two-axis movements were considered as demands, the same classification was also applied to all the needs except the user friendly, ease of manufacture and ease of assembly which were considered as

wishes. The second phase was to generate design concepts, then select one of them. The specifications were identified based on the customer needs. Other steps in PDP were implemented with system-level design then detail design. Drafts were generated for the mechanical system parts using CAD. The mechanical system can achieve the rotation movement by using castor and rotating base plates which have multiple holes in them to secure the desired rotation angle by placing a bolt and nut in them. The tilting movement mechanism was achieved by having two plates with holes and slit in them. These two plates were shaped as the letter D. The parallel D-plates were attached to the SuperStruts assembled to T-Slot Channel, which holds the PV panel. The D-plates were also attached to the main vertical column through a bolt and nut. This center bolt is the pivot of rotation for the main block that contains the PV panel and with this rotation the tilting movement is achieved. Four sand blocks were also used on the four base square tubes that attached to the rotating base plate. The final stages of the PDP were testing and refinement plus production. The manufacturing labs in Texas State University were used to produce the mechanical system. Many pieces of equipment and technologies were used including waterjet machine, welding, chop saw, and 3D printer.

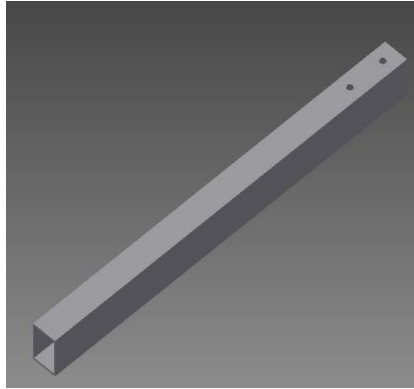


Figure 26. Square tube draft. CAD draft of the square tube; used for the legs in the mechanical system.

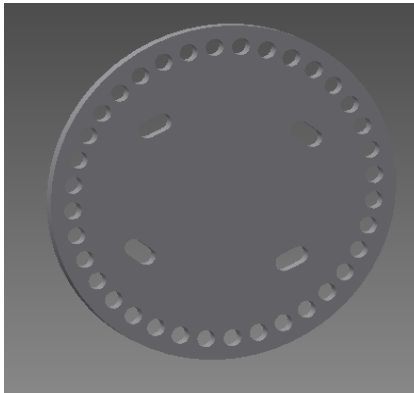


Figure 27. Base plate draft. CAD draft of the base plate for rotation in the mechanical system

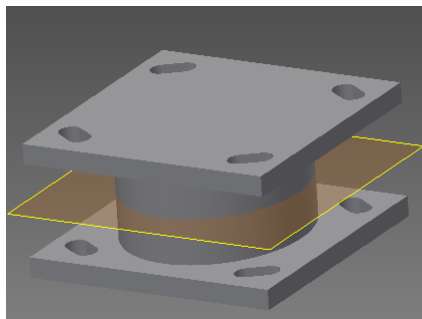


Figure 28. The caster draft. CAD draft of the caster for spin mechanism in the mechanical system



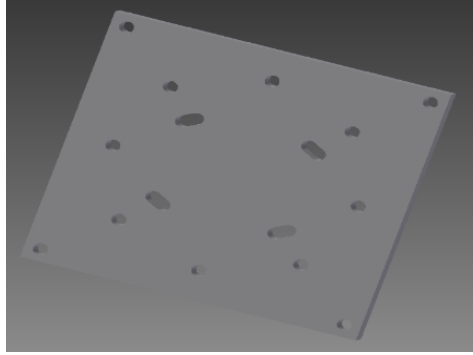


Figure 29. Fixed base plate. CAD draft of the fixed base plate in the mechanical system.

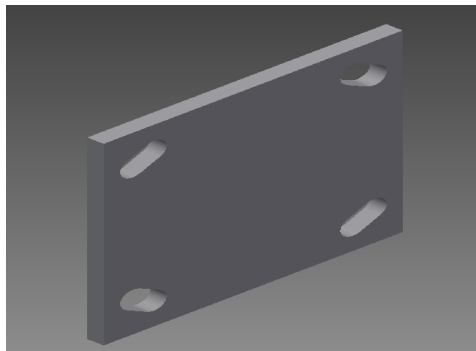


Figure 30. Square tube adaptor plate. CAD draft of the square tube adaptor plate in the mechanical system.

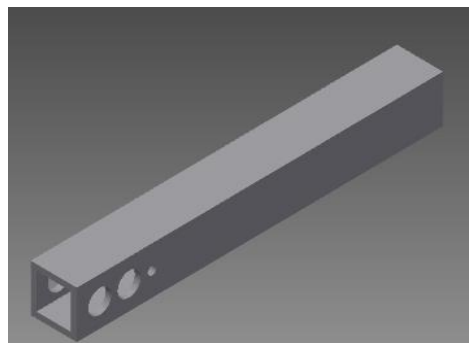


Figure 31. Square tube column. CAD draft square tube column in the mechanical system.

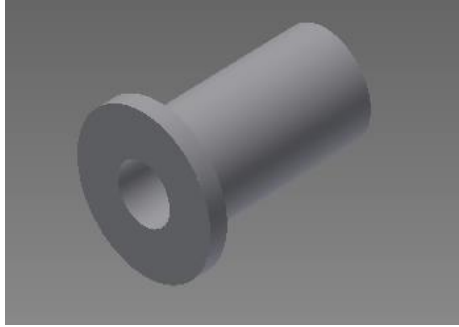


Figure 32. Sweeping mechanism pin. The CAD draft of the sweeping mechanism for D-Plate in the mechanical system.

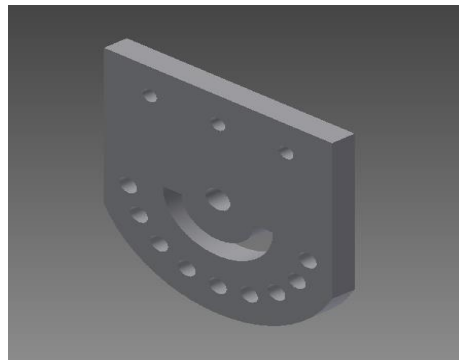


Figure 33. D-plate draft. CAD draft of the D-plate tilt mechanism in the mechanical system.

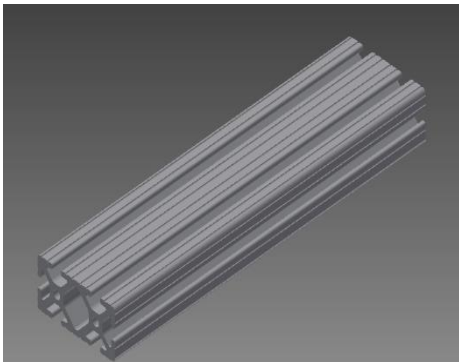


Figure 34. T-slot bar .CAD draft of T-slot for tilt mechanism in the mechanical system.

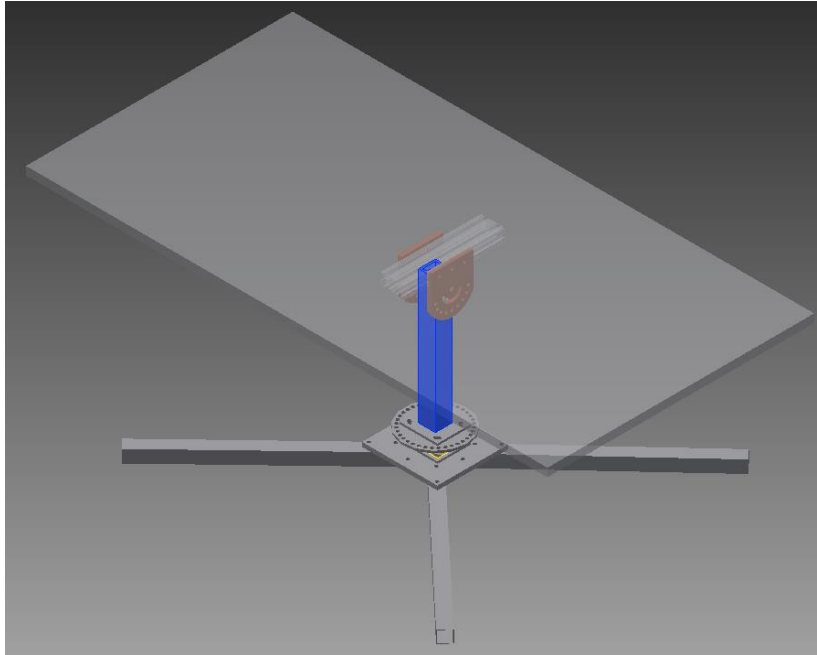


Figure 35. The final assembly draft. The final assembly of the mechanical system generated with Inventor Autodesk.

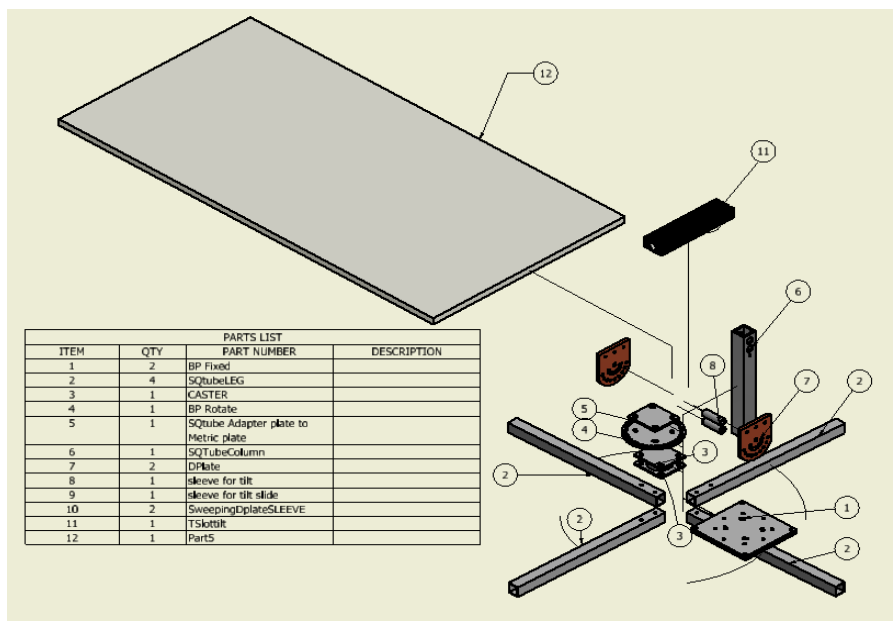


Figure 36. Parts draft and list. Parts draft and list generated by Inventor Autodesk.

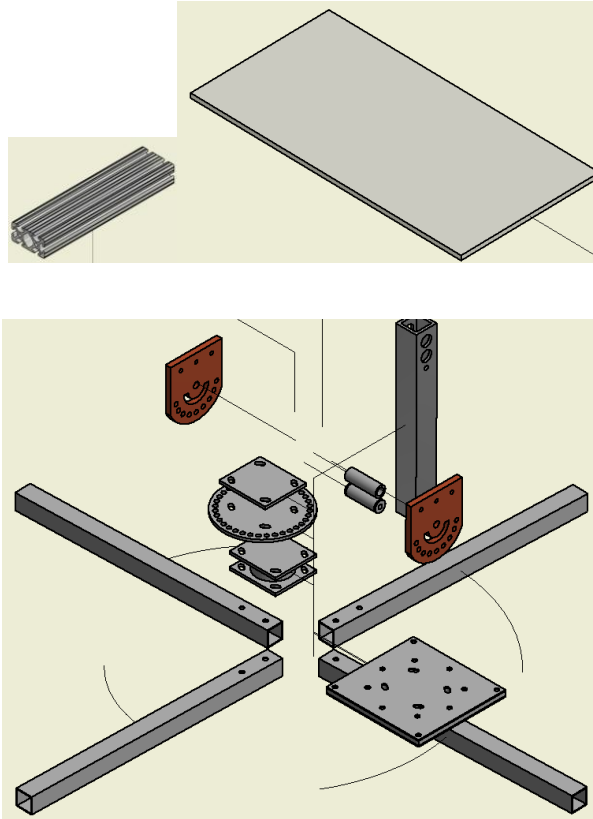


Figure 37. Various parts draft and how to assemble.



Figure 38. Water jet machine used in the production.



Figure 39. 3D printer used in the production.

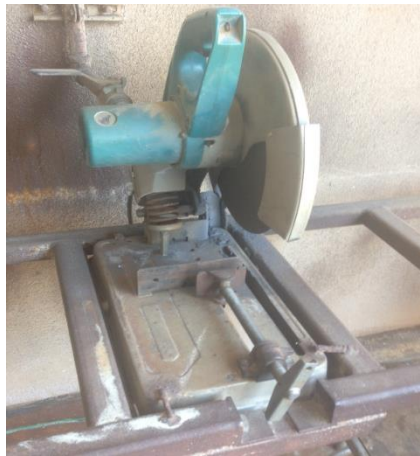


Figure 40. Chop saw used in the production.



Figure 41. SuperStruts. It is assembled to T-Slot Channel. This structure used to hold the PV panel.



Figure 42. The rotating base plate used in the mechanical system.

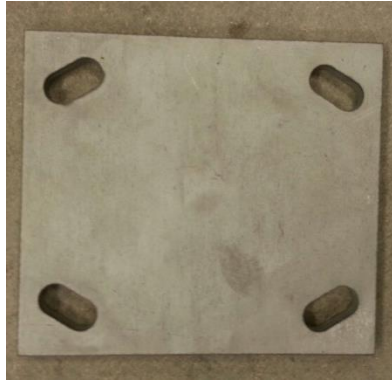


Figure 43. The square tube adaptor base used in the mechanical system.



Figure 44. The square steel legs assembled to fixed base plate and caster.

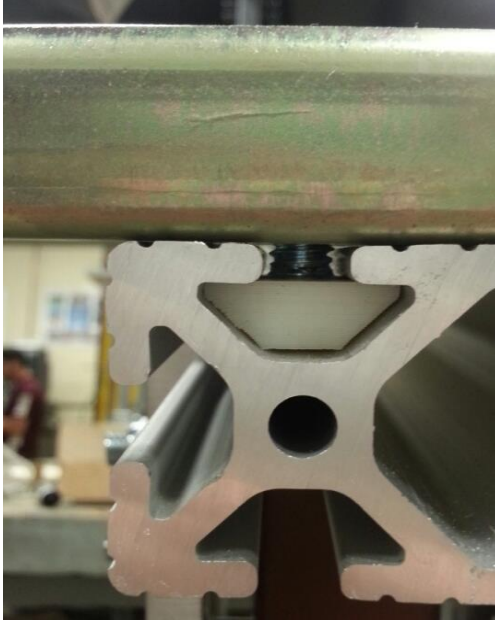


Figure 45. The T-slot plastic bolt adaptor used in the mechanical system.



Figure 46. The D-plate with several tilt angle settings.





Figure 47. The two D-plates attached to the PV panel holder structure.

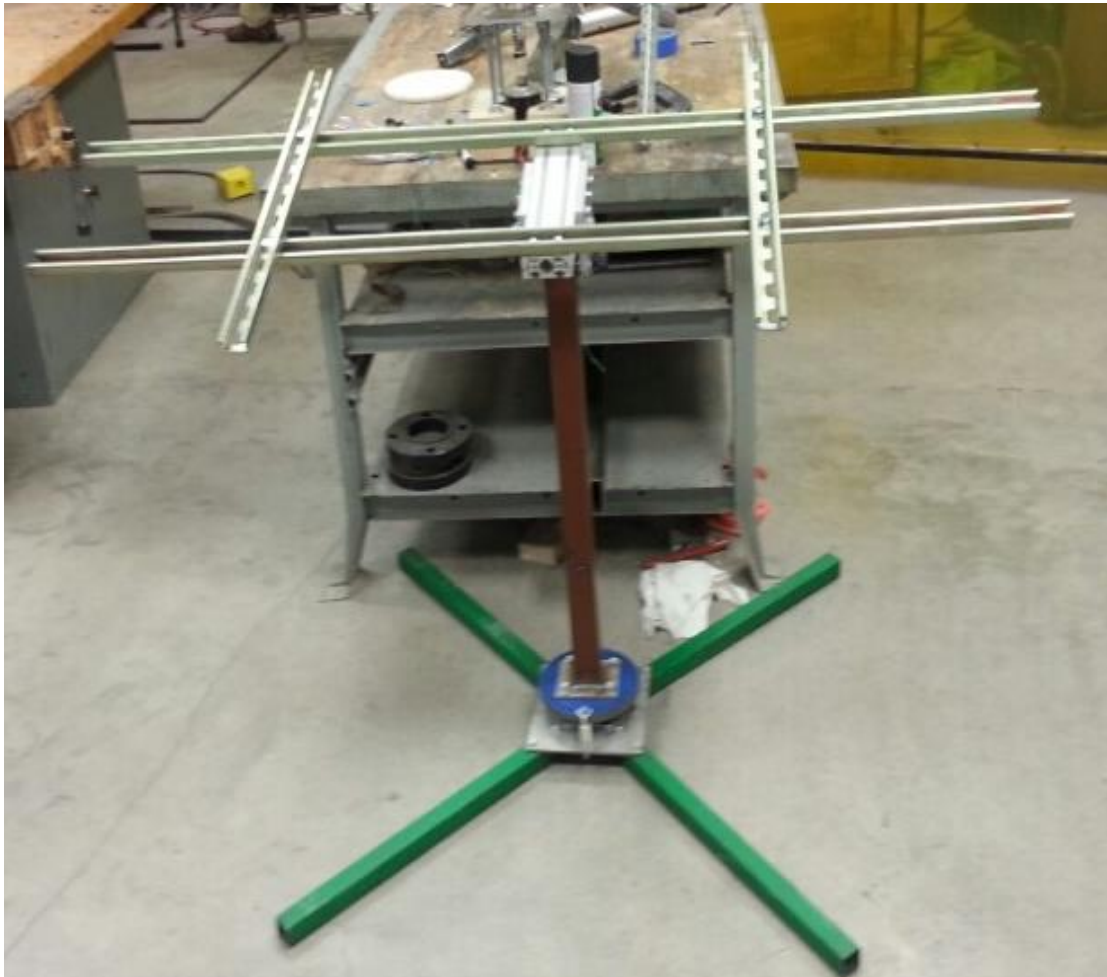


Figure 48. The final assembly of the mechanical system.



Finally the following table is shows the bill of materials (BOM) and the cost for the mechanical system.

Table 6. Bill of materials.


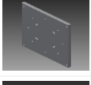
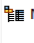




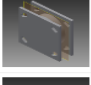
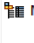













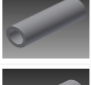


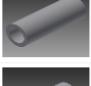


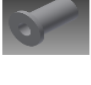


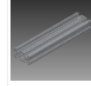




Bill of Materials [SPASSEMB.iam]										
Model Data Structured Parts Only (Disabled)										
Item	Part Number	Thumbnail	BOM Structure	Unit	QTY	QTY	Stock Number	Description	Re	
	1 BP Fixed		 Normal	Each	2					
	2 SQtubeLEG		 Normal	Each	4					
	3 CASTER		 Normal	Each	1					
	4 BP Rotate		 Normal	Each	1					
	5 SQtube Adapter plate to Metric plate		 Normal	Each	1					
	6 SQTubeColumn		 Normal	Each	1					
	7 DPlate		 Normal	Each	2					
	8 sleeve for tilt		 Normal	Each	1					
	9 sleeve for tilt slide		 Normal	Each	1					
	10 SweepingDplateSLEEVE		 Normal	Each	2					
	11 TSlottilt		 Normal	Each	1					
	12 Part5		 Normal	Each	1					

Table 7. Parts list.

Part	Cost	Purchase Place	Material
Caster	\$58.76	Amazon	Steel
T-Slot Extrusion	\$24.22	Amazon	Aluminum
1 ½ " Square Tube Legs (8ft)	\$14.26	Metals4U	Hot rolled Steel
Half Slot 14 gage SuperStrut (20ft)	\$35.50	Lowes	Galvanized Steel
D-plate Tilt Mechanism (x2)	\$0.00	University Inventory	Aluminum
Rotating base plate	\$0.00	University Inventory	Steel
Fixed Base Plate	\$0.00	University Inventory	Steel
Square Tube Adaptor Plate	\$0.00	University Inventory	Steel
Square Tube Column	\$0.00	University Inventory	Steel
Bolts	\$3.17	Lowes and University Inventory	Zinc coated Steel
Sweeping Mechanism For D-Plate	\$0.00	University Inventory	Plastic and Steel
Total Spent	<b>\$135.91</b>	Budget	\$125.00
Market Value	\$250.00	Market Value Savings	<b>\$114.09</b>

## VI. RESPONSE SURFACE METHODOLOGY

### Introduction

The experiment was designed using Response Surface Methodology (RSM). The selection of the method was based on both the objective of the experiment and the number of factors and levels. RSM can be defined as a combination of mathematical and statistical techniques effective for establishing, refining, and optimizing processes. It can be also used for the design and creation of new products as well as improving current ones (Myers & Montgomery, 2002). The RSM inputs are the identified independent variables and the output will be the yield response which represents the performance measure of the process. The unknown response can be approximated to a first, second or third order model. The most used model is the second order model (Quadratic) especially if curvature in the response is suspected. In this model main effects and interaction between factors can be identified. In general, the second-order model is:

$$\eta = \beta_0 + \sum_{j=1}^k \beta_j x_j + \sum_{j=1}^k \beta_{jj} x_j^2 + \sum_{i < j} \beta_{ij} x_i x_j$$

Where:

$x_j$  : Variable j

$\beta_0, \beta_j, \beta_{jj}$  : Parameters of second-order model

$\eta$  : Model response

Variables ( $x_j$ ) usually are coded variables transformed from natural variables. The independent variables are called natural variables when they are expressed with natural

units. "...Natural Variables can be transformed to coded variables which are dimensionless with mean zero and the same spread or standard deviation" (Myers & Montgomery, 2002, p.3).

An experiment, as described by Montgomery (1997), is a test or sequence of tests where deliberate adjustments are made to the input variables of a system so that we may detect and distinguish the causes for the changes in the output response. Designed experiments are used in many disciplines and their impacts can be seen in almost every aspect of our lives. They help to build our knowledge about certain processes and systems which give us insight to enhance and improve performance. Engineering fields are one of the biggest venues where design of experiment is used. Lower costs, new ideas, new processes, new products, and new systems are invented due to the practice of design of experiments.

### **Factors Identification**

The first stage of the Response Surface Methodology is to identify the important factors and their levels. They should have significant impact on the yield response. In this experiment independent variables with multi levels are identified with a goal to study their effect on the response yield and to find the optimum setting of the factors' levels. A model of typical process is applied with input, independent variables, uncontrollable factors, and output. The photovoltaic effect is considered as the process. Two PV panels are used as the input materials. The irradiance is considered another input to the process. The date, time, and location were also considered as inputs to the process. The temperature of the PV panels and the ambient temperature, though measured, were considered as uncontrollable factors. General weather conditions were considered as

uncontrollable factors including the clouds and humidity. Tilt angle, azimuth angle, wind intensity, and solar panel cleanness were considered as the controllable factors.

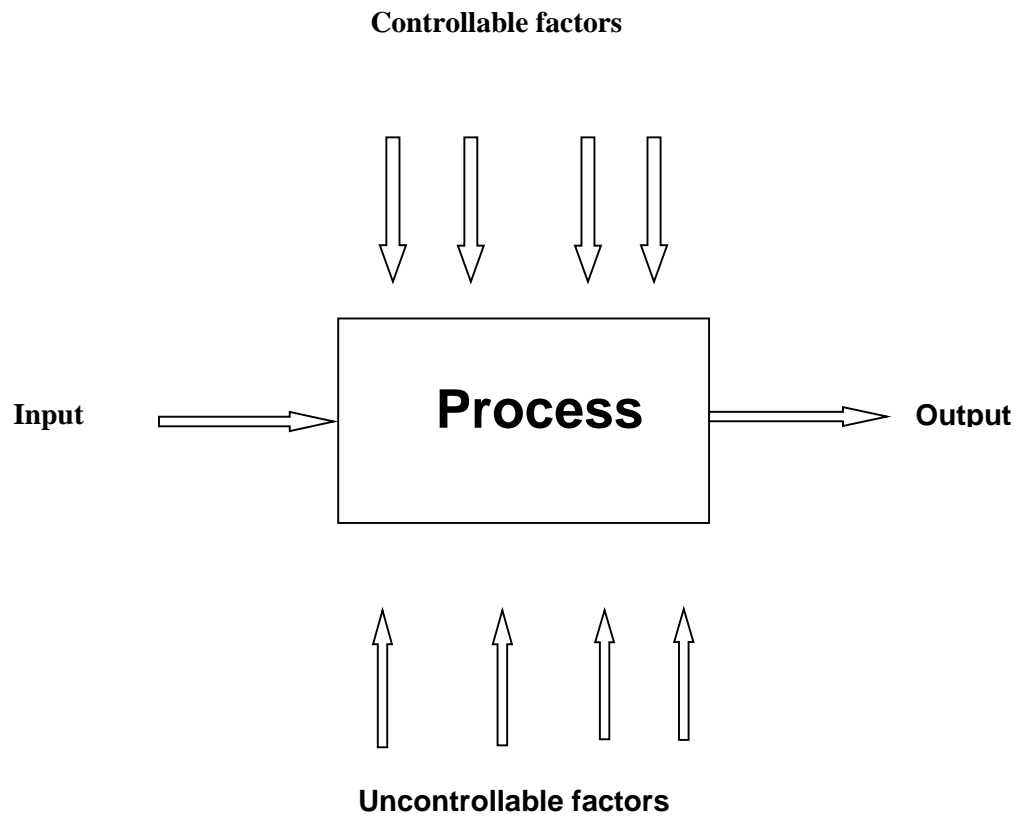


Figure 49. General model of a process or system. Adapted from “Design and analysis of experiments” by D. Montgomery, (1997) p. 2

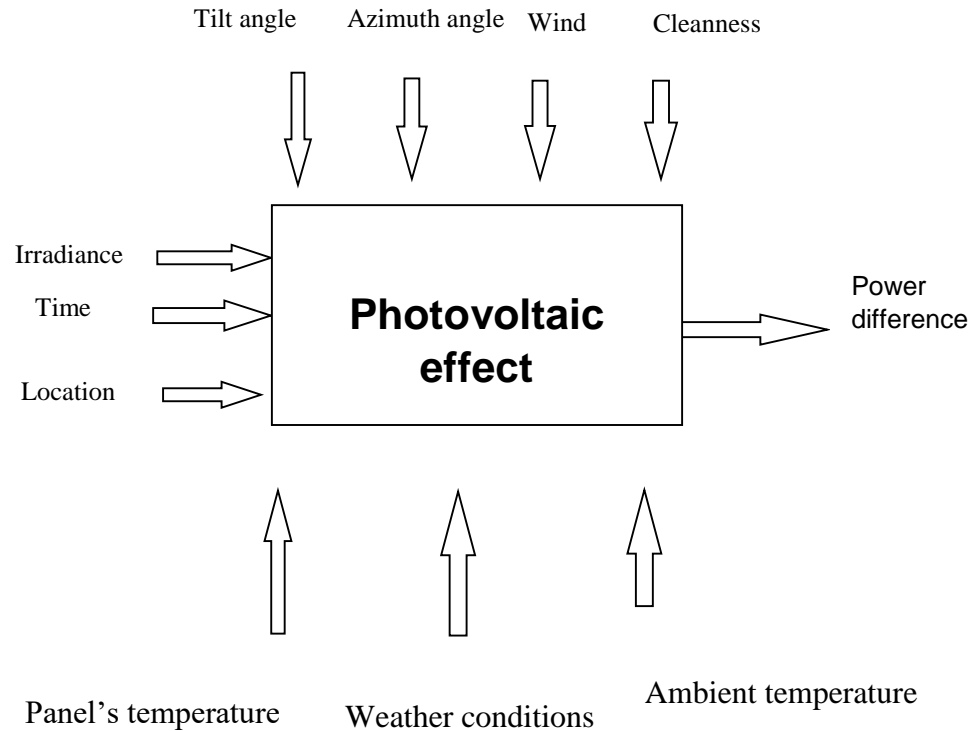


Figure 50. The process diagram of the experiment.

### Factor Levels in Feasible Ranges

For four independent variables three levels in the feasible ranges were identified: A-tilt angle with three levels of 0°, 30°, and 60° from the horizon; B- azimuth angle with three levels of 0°, 45°, and -45° from the south; C- the wind with three levels of 0, 5.5, and 10 Km/h. The wind factor has been achieved through the use of a fan with multiple speeds. The speed of the fan was measured through the use of a wind sensor. The fan was placed in front of the panel with two feet distance from the center of the PV panel. The fan was set to oscillate to make the air waves cover the entire PV panel. Finally, D- the cleanness of the PV panels with three levels. Talc was used to emulate the cleanness of

the PV panels. Three levels of cleanness were determined based on the amount of the talc scattered randomly on the surface of the PV panel. The levels were absence of talc as 0 gram, ten shakes of talc which equal 20 grams as second level, and the third level of cleanness was twenty shakes of talc which is equal to 40 grams.

The two PV panels used in the experiment were identical. One panel was placed on the dual axis mechanical system while the other was flat on the ground. The rheostats loads that were used in the electrical system were identical. To overcome the minor discrepancy of the initial output power of the two PV panels, a small calibration was applied to them with  $R1=7.1\Omega$  and  $R2=7.4\Omega$ . The irradiance of the flat PV panel was determined as the input of the process and it was measured through the use of an irradiance sensor placed flat beside the flat PV panel. Another irradiance sensor was attached to the mechanical system and it was subjected to only two factors which were tilt and azimuth angles (orientation of the PV panel), and their three levels. The second sensor was recording the irradiance changes due to the changes in the tilt angles and the azimuth angles. The yield response of the process was determined to be the recorded power differences between the two PV panels. The selection of the power difference as an output was to minimize the effect of the variation of the irradiance during the experiment on the process. The four factors were selected with high, mid, and low levels.

Table 8. The four uncoded factors with their three levels.

level	A=Tilt Angle (degree from horizon)	B=Azimuth angle (degree from south)	C=wind (Km/h)	D=Panel Cleanness (grams of talc)
Low	0	-45	0	0
Mid	30	0	5.5	20
High	60	45	10	40

Table 9. The four coded factors with their three levels.

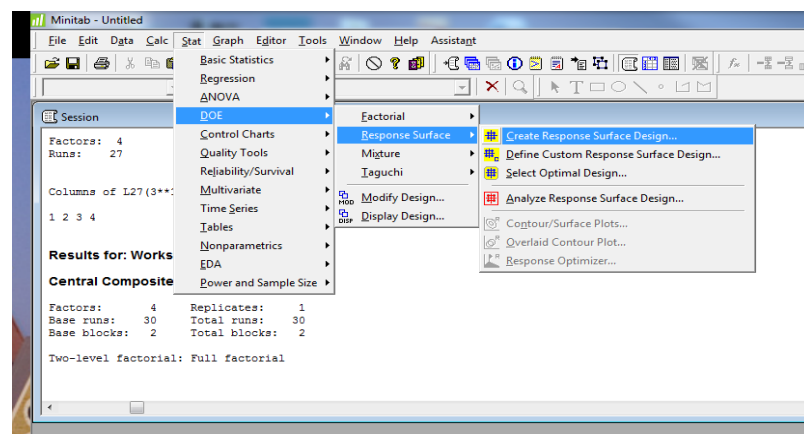
level	A	B	C	D
Low	-1	-1	-1	-1
Mid	0	0	0	0
High	1	1	1	1



## Design of Experiments

Experimental design has been implemented to characterize the process in terms of how input parameters affect the power output. The main two kinds of designs of Response Surface are Central Composite designs and Box-Behnken designs. The selection of the type of Response Surface design is the second stage. In this experiment Box- Behnken was used. The advantages of using Box-Behnken designs are a) to have less design points than Central Composite designs which will make it less costly, and b) high efficiency to estimate the first and second order model coefficients. The disadvantages are the incapability to use runs from factorial experiments, the limitation of three levels per factor while the Central Composite can have up to five, and finally they cannot have runs with the extreme value of the factors ("What Is A Response Surface Design? – Minitab, n.d.").

The software used for the design of experiment and to analyze the result is Minitab. The setting included the selection of three replications and randomization to reduce the bias. The software generated the following 81 uncoded runs.



Figurer 51. Minitab. Using Minitab Graphic user interface (GUI) to create RSM design of experiment.

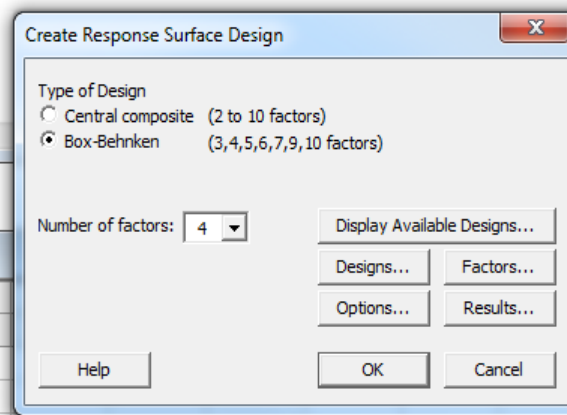


Figure 52. Using Minitab to create Box-Bhenken design of RSM.

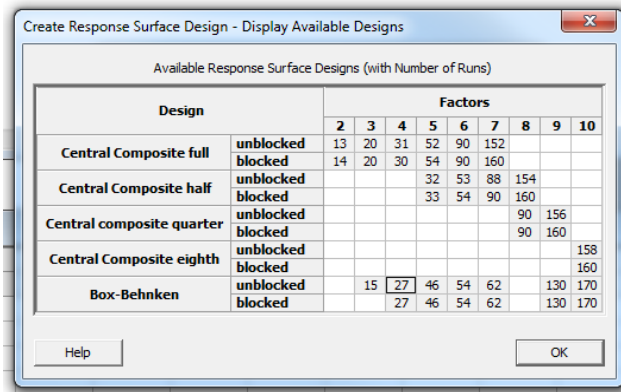


Figure 53. Using Minitab GUI to select unblocked Box-Bhenken runs.

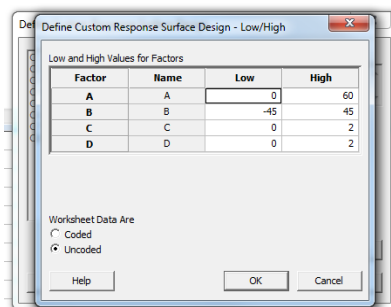


Figure 54. Using Minitab GUI to identify the high and low levels for each factor.

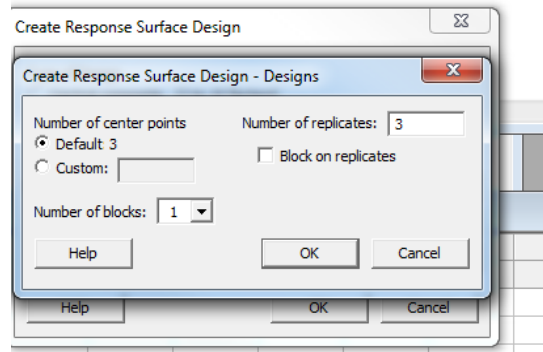


Figure 55. Using Minitab GUI to select the design specifications.

### Conducting the Experiments

The experiment was conducted on the 17<sup>th</sup> and the 18<sup>th</sup> of December 2015. The readings were collected from the data acquisition system and were inputted to the runs' charts. These runs were later compared to the data saved in the system to guarantee the accuracy.

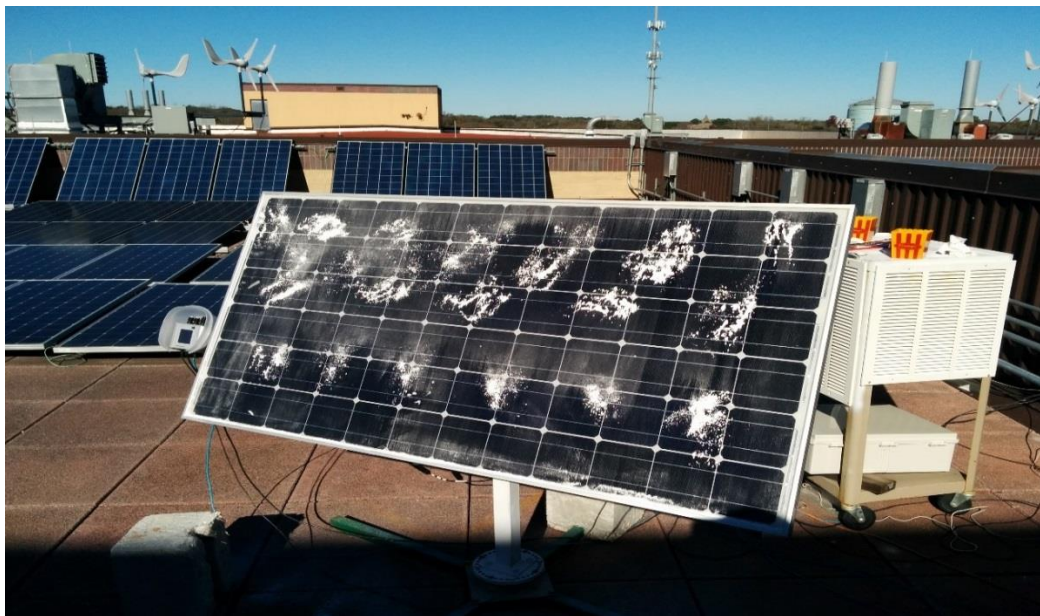


Figure 56. The PV panel with levels of treatments. The tilt at 60°, the panel toward the south, the wind at 0, and low level of cleanness.



Figure 57. The PV panel subjected to the treatment during the experiment. The tilt at  $0^\circ$ , the panel toward the east, the wind at 0, and mid-level of cleanness.

Appendixes B, C, and D show the runs, data, and some efficiency calculations.

## Data Analysis

The next stage of the RSM is to analyze the data and find the RSM coefficients. Minitab is used to perform the aforementioned tasks. The confidence level used during the analysis was 95%, and it was two sided.

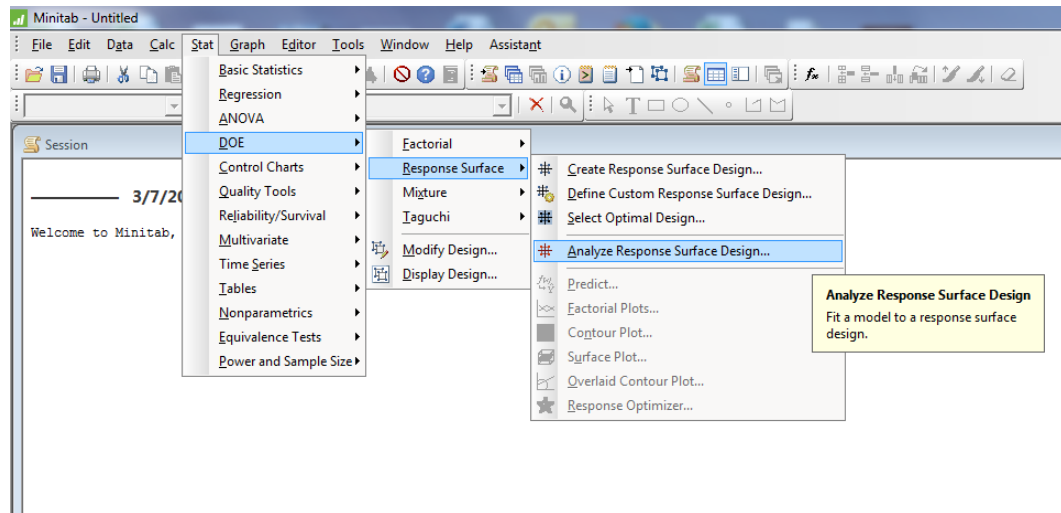


Figure 58. Using the Minitab GUI to analyze the results.

The following results of the analysis were found.

Table 10. The analysis of the data using Minitab.

## Response Surface Regression: Power Difference versus A, B, C, D

### Analysis of Variance

Source	DF	Adj SS	Adj MS	F-Value	P-Value
Model	14	117742	8410.2	16.19	0.000
Linear	4	102326	25581.4	49.24	0.000
A	1	45412	45411.6	87.42	0.000
B	1	2604	2604.4	5.01	0.029
C	1	91	90.6	0.17	0.678
D	1	54219	54219.1	104.37	0.000
Square	4	9361	2340.2	4.50	0.003
A*A	1	2188	2188.2	4.21	0.044
B*B	1	2071	2071.3	3.99	0.050
C*C	1	254	253.7	0.49	0.487
D*D	1	2327	2327.0	4.48	0.038
2-Way Interaction	6	6056	1009.3	1.94	0.087
A*B	1	2033	2033.2	3.91	0.052
A*C	1	377	377.4	0.73	0.397
A*D	1	161	160.6	0.31	0.580
B*C	1	2617	2616.7	5.04	0.028
B*D	1	4	4.1	0.01	0.930
C*D	1	864	863.6	1.66	0.202
Error	66	34286	519.5		
Lack-of-Fit	10	7254	725.4	1.50	0.163
Pure Error	56	27032	482.7		
Total	80	152028			

### Model Summary

S R-sq R-sq(adj) R-sq(pred)  
22.7920 77.45% 72.66% 66.19%

### Coded Coefficients

Term	Effect	Coef	SE Coef	T-Value	P-Value	VIF
Constant		23.78	7.60	3.13	0.003	
A	71.03	35.52	3.80	9.35	0.000	1.00
B	17.01	8.51	3.80	2.24	0.029	1.00
C	3.17	1.59	3.80	0.42	0.678	1.00
D	-77.62	-38.81	3.80	-10.22	0.000	1.00
A*A	-23.39	-11.69	5.70	-2.05	0.044	1.25
B*B	-22.76	-11.38	5.70	-2.00	0.050	1.25
C*C	-7.96	-3.98	5.70	-0.70	0.487	1.25
D*D	24.12	12.06	5.70	2.12	0.038	1.25
A*B	26.03	13.02	6.58	1.98	0.052	1.00
A*C	-11.22	-5.61	6.58	-0.85	0.397	1.00
A*D	-7.32	-3.66	6.58	-0.56	0.580	1.00
B*C	-29.53	-14.77	6.58	-2.24	0.028	1.00
B*D	-1.17	-0.58	6.58	-0.09	0.930	1.00
C*D	-16.97	-8.48	6.58	-1.29	0.202	1.00

### Fits and Diagnostics for Unusual Observations

Obs	Power Difference	Fit	Resid	Std Resid	R
4	88.40	39.60	48.80	2.39	R
21	46.00	102.13	-56.13	-2.74	R
54	76.70	23.78	52.92	2.46	R
66	2.00	60.59	-58.59	-2.86	R

R Large residual

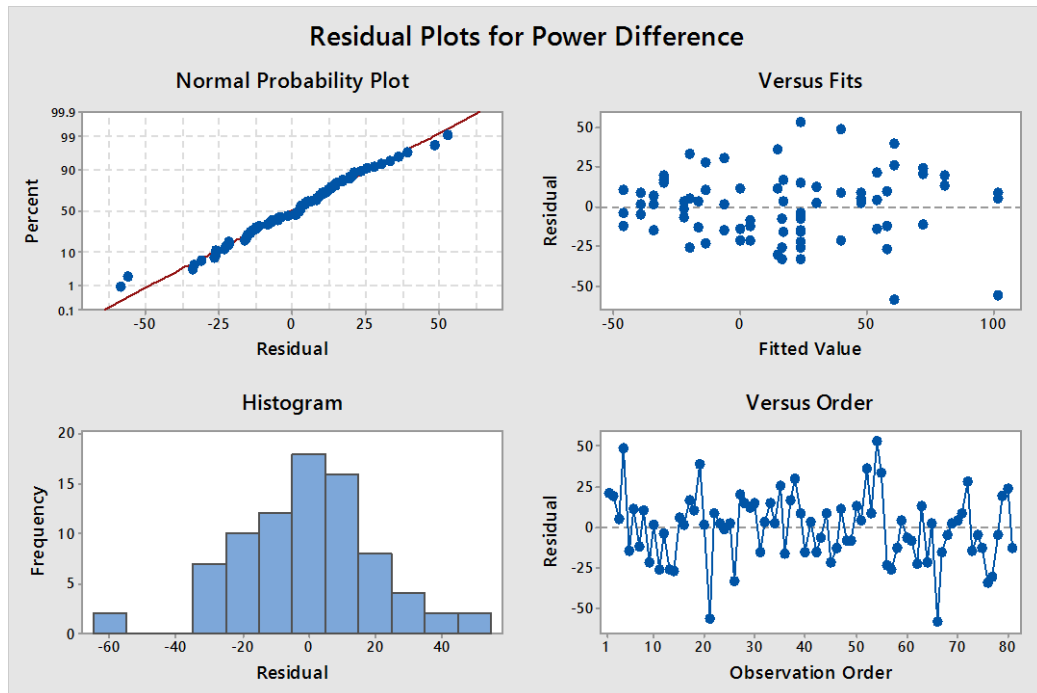


Figure 59. Four-in-one residual plot generated by Minitab.

The normal probability plot on the top left of figure 59 shows normal distribution of the residuals. The histogram plot in the same figure shows the frequency of the residual. The highest residual frequency is around zero. Unusual high residuals (-60) can be seen with low frequency. The residual versus fits plot shows no pattern which supports the regression model. The residual versus observation order shows randomization which supports the independence assumption.

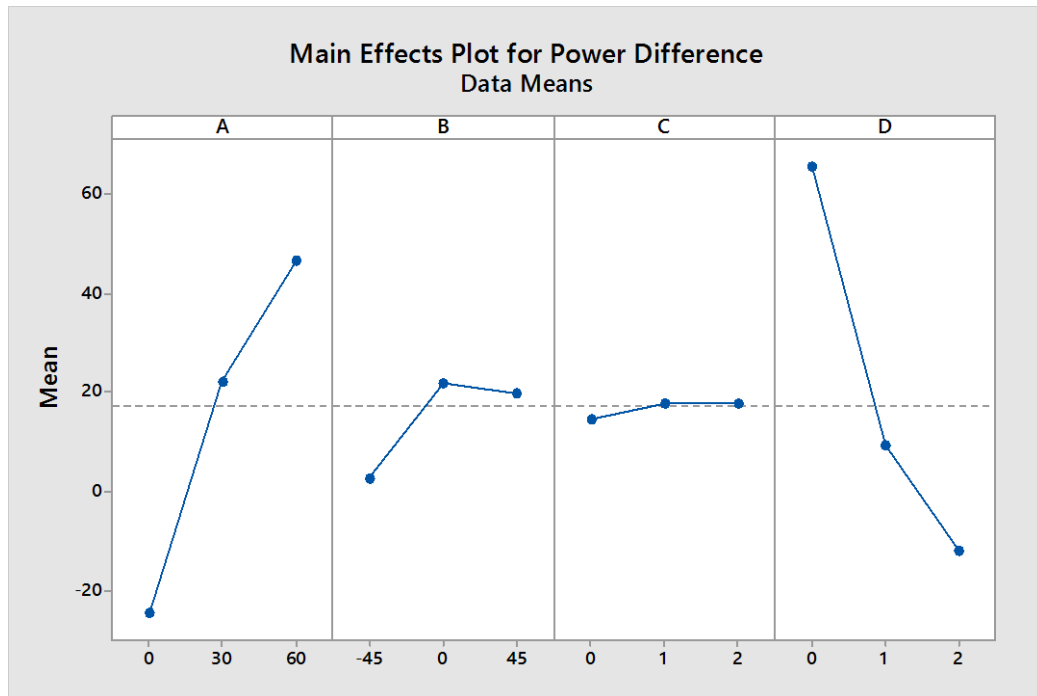


Figure 60. The main effect plot generated using Minitab for the yield response.

The main effect plot for the response indicates that the 60 ° angle of tilt produces the highest output, while the zero degree gives the lowest for this season of the year. The same plot shows zero degree azimuth angle (orientation of the PV panel) gives the highest response while -45° gives the lowest. The response yielded to 45 ° is close to the zero degree of the azimuth angle for this season. The same plot shows almost the same response for the three levels of treatment of the wind. Finally the clean panel with no talc gives the highest yield response. The response is decreasing with the increment of the talc on the subjected panel.



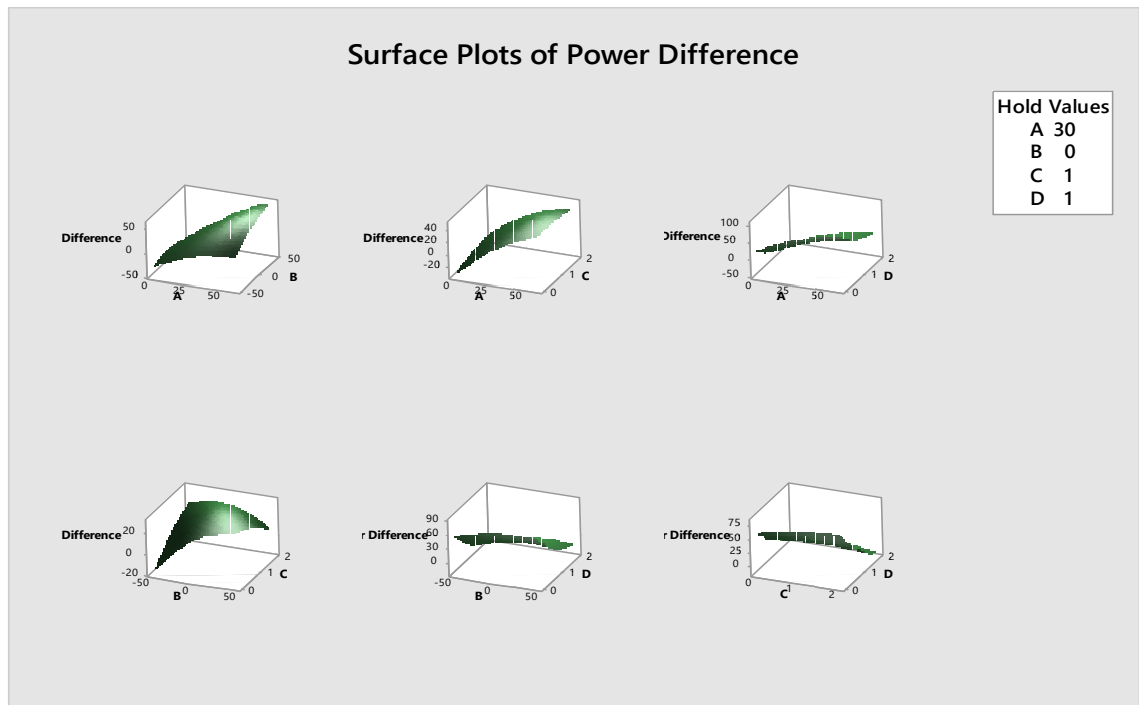


Figure 61. The surface plot of the yield response as generated using Minitab.

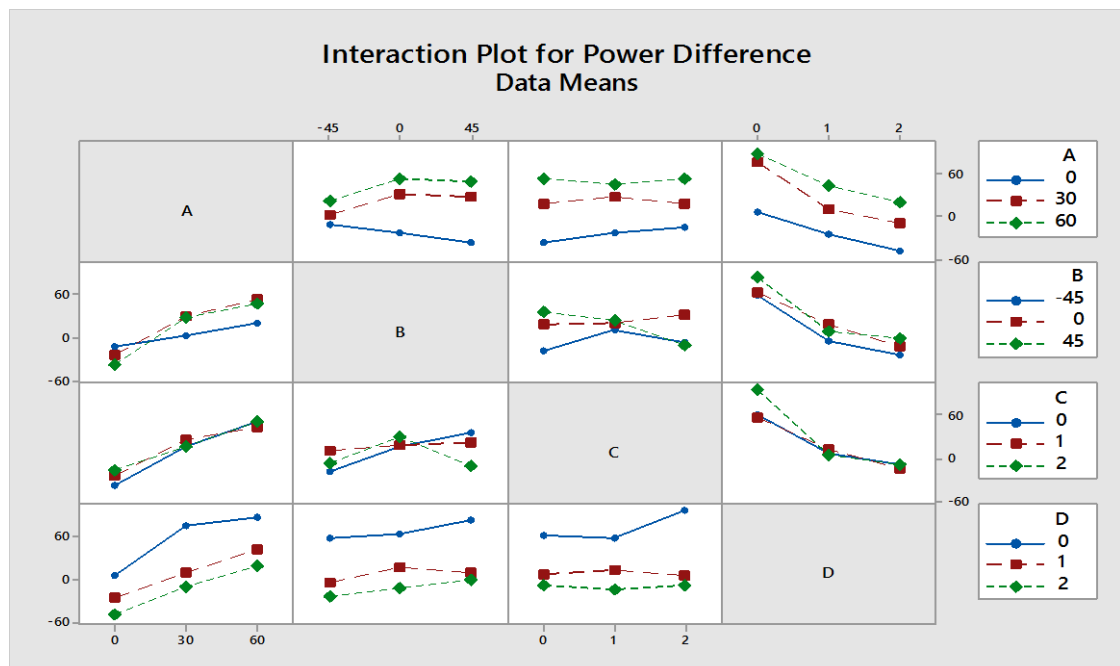


Figure 62. The interaction plot. The interaction plot for the yield response with the four factors and their three levels as generated using Minitab.



Figure 63. Contour plot of the yield response. The plot shows the levels of two factors at a time with corresponding response.

The yield response equation calculated by Minitab through Regression.

The Regression Equation in Uncoded Units is

$$\begin{aligned}
 \text{Power Difference} &= 4.1 + 2.272 A + 0.241 B + 23.6 C - 50.8 D - 0.01299 A^2 \\
 &- 0.00562 B^2 - 3.98 C^2 + 12.06 D^2 + 0.00964 AB - 0.187 AC \\
 &- 0.122 AD - 0.328 BC - 0.013 BD - 8.48 CD
 \end{aligned}$$

The Regression Equation in coded Units is

$$\begin{aligned}
 \text{Power Difference} &= 23.78 + 35.52 A + 8.51 B + 1.59 C - 38.81 D - 11.69 A^2 - \\
 &11.38 B^2 - 3.98 C^2 + 12.06 D^2 + 13.02 AB - 5.61 AC - 3.66 AD - 14.77 BC - \\
 &0.58 BD - 8.48 CD
 \end{aligned}$$

The calculated P-values through the ANOVA indicate the significance of the factors and their interactions on the yield response. Some of the factors have a high P-value and they were removed from the edited equation (higher than 0.05). These factors or their interactions are: C, C<sup>2</sup>, AC, AD, BD, and CD. Some of the second order parameters have a critical P-value and are kept in the final equation. These include BB and AB with a P-value equal to 0.05 and 0.052 respectively. The wind factor and its interactions showed insignificant impact on the response except the interaction with the azimuth angle (orientation) of the PV panel. This might be due to uncontrollable natural wind occurring during the experiment.

The final equations are

Regression Equation in Uncoded Units.

*Power Difference*

$$= 4.1 + 2.272 A + 0.241 B - 50.8 D - 0.01299 A^2 - 0.00562 B^2 + 12.06 D^2 + 0.00964 AB - 0.328BC$$

Regression Equation in Coded Units.

$$Power\ Difference = 23.78 + 35.52 A + 8.51 B - 38.81 D - 11.69 A^2 - 11.38 B^2 + 12.06 D^2 + 13.02 AB - 14.77 BC$$

## Optimization

The optimization of the response was determined through the use of Minitab. The software generated the optimum settings of the factors to maximize the yield response.

The following table and figure show the Minitab-generated optimum results.

Table 11. Minitab optimization results.

**Response Optimization: Power Difference**

Parameters

Response	Goal	Lower	Target	Upper	Weight	Importance
Power Difference	Maximum	-59.2	110.8		1	1

Starting Values

Variable	Setting
----------	---------

A	0
B	0
C	0
D	0

Solution

Solution					Power Difference	Composite Desirability
	A	B	C	D	Fit	
1	60	45	0	0	119.178	1

Multiple Response Prediction

Variable	Setting
----------	---------

A	60
B	45
C	0
D	0

Response	Fit	SE Fit	95% CI	95% PI
Power Difference	119.2	20.1	(79.0, 159.3)	(58.5, 179.9)

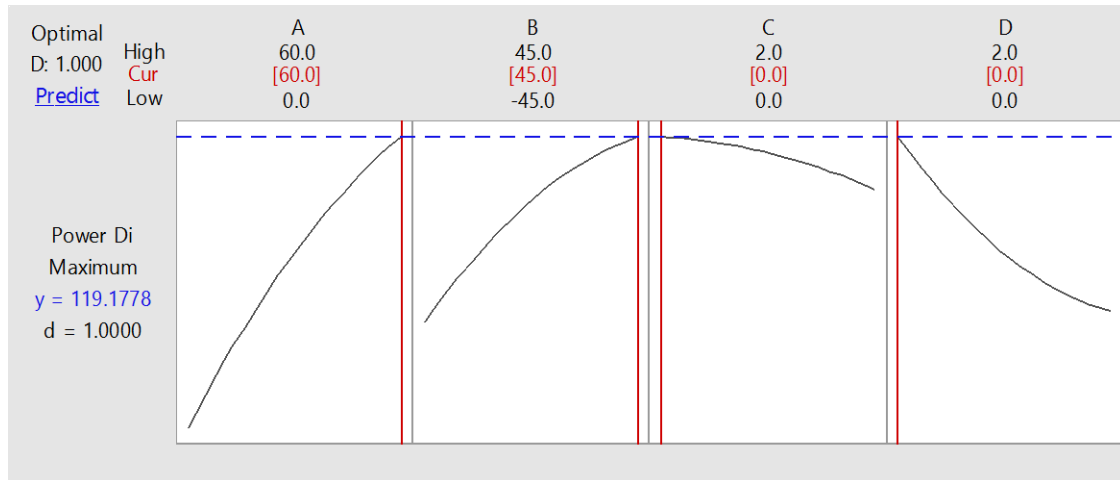


Figure 64. The optimization graph generated by Minitab. The four factors and their optimum setting is shown in red.

The Minitab calculations shows that the optimum settings to maximize the power difference are achieved when the tilt of the PV panel is 60° and the PV panel is oriented toward the west and there is no wind and no dirt on the surface of the panel.

### Investigation the Sun's Position and Its Effect on the Optimum Point

One element which was ignored during the study and optimization process is the fact that sun's position was changing during the data collection of the experimental runs. It is obvious the optimum position for tilt and azimuth is when PV is pointed exactly toward the sun (continuous sun tracking). However for the fixed level settings and since conducting experiments may take several hours, assuming a fixed position for the sun is inaccurate. Further investigation of the data showed that the optimum point for the tilt angle changes simply by changing the time of the day when the runs were conducted. To show this effect, in this study, the experiment was conducted during two consecutive days, the 17th and 18th of December. Mid-day on these two days was around 12:28 PM.

The runs were divided into two groups, before and after mid-day. The runs before mid-day were 22 runs with the following run orders [1 to 5, and 42 to 58] and after mid-day were 59 runs with the following run orders [6 to 41, and 59 to 81]. The main effect plots were generated using Minitab for each group. The maximum power differences for the runs before mid-day were achieved with the PV panel oriented toward the east. The maximum power differences for the runs after mid-day were achieved with the PV panel toward the west. This shows the significant importance of tracking the sun for the PV panel.

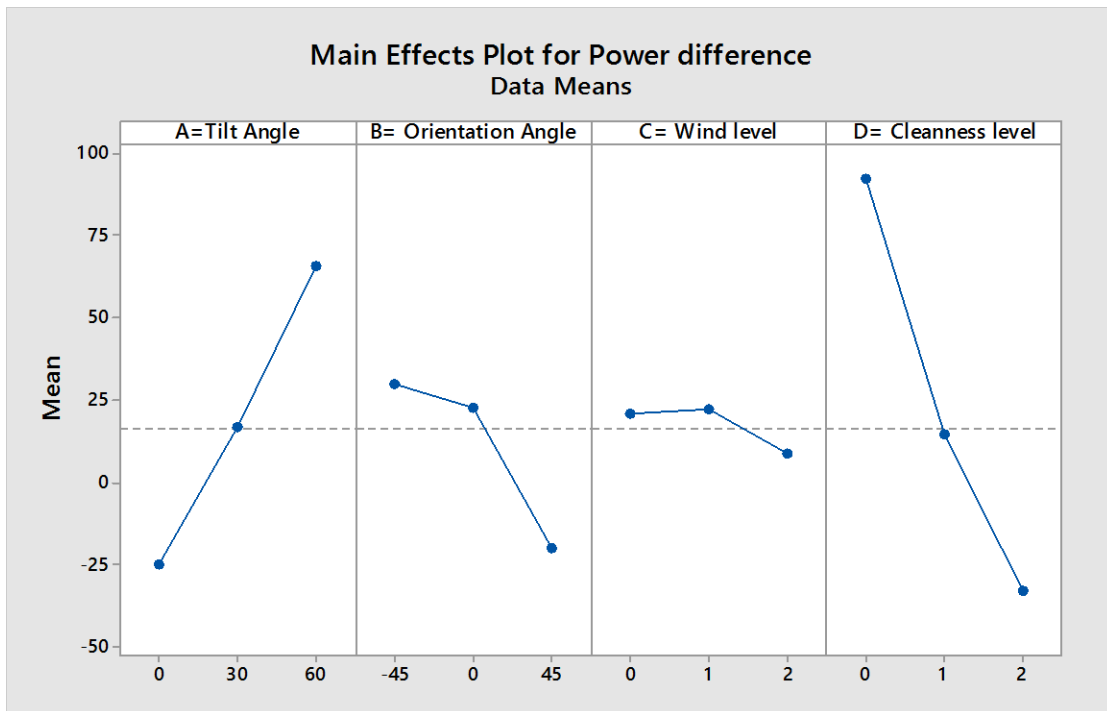


Figure 65. The main effect for the runs before mid-day. The highest achieved response is when the PV panel is pointed toward the east.

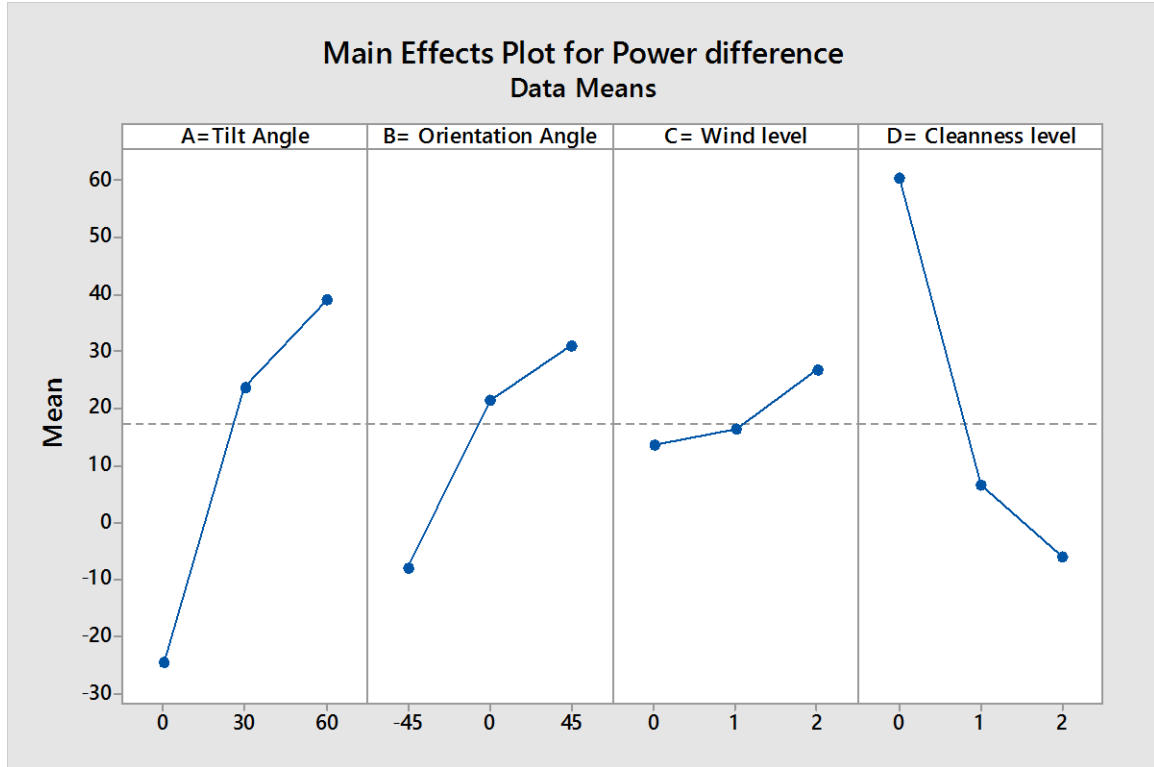


Figure 66. The main effect plot for the runs in the afternoon. The highest achieved response is when the PV panel is pointed toward the west.

### Efficiency Calculations

The efficiency of both PV panels were calculated. The efficiency equation is

$$\eta = \frac{(P_{out} \div A)}{(P_{in} \div A)} * 100$$

Where:

P is power and A is the area of the PV panel.

$$A = 1.11502347 \text{ m}^2.$$

The first PV panel was the panel which was subjected to the manipulations. The efficiencies of this PV panel were calculated for all runs once with irradiance1 as input and later with irradiance2. The second PV panel is the flat panel. The efficiencies calculations were done with the irradiance2 as the input. The irradiance gains are also calculated for all runs.

$$\text{Irradiance gain} = \text{Irradiance 1} - \text{Irradiance 2}$$

The flat PV panel efficiency was relatively constant, while the first PV panel efficiency was affected with the treatment levels.

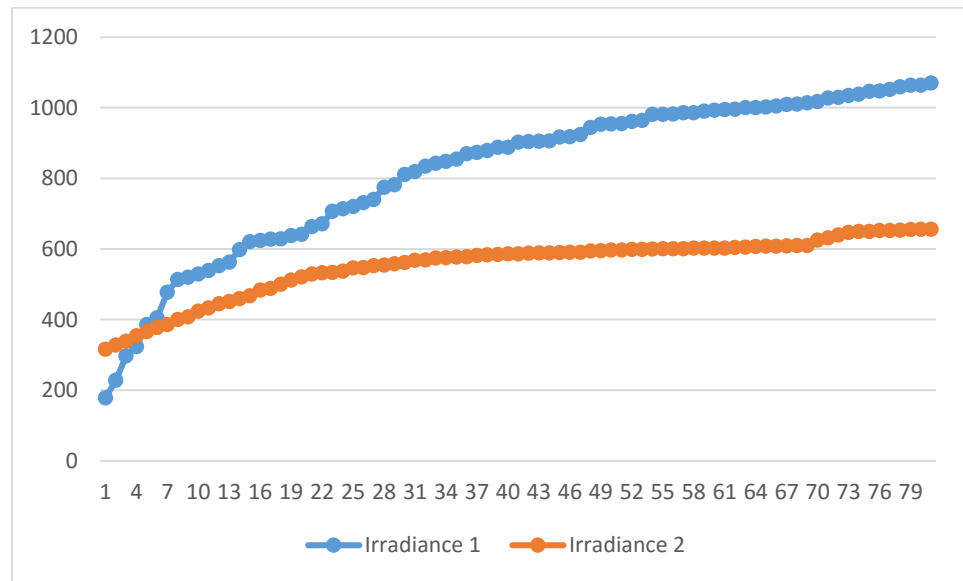


Figure 67. The received irradiance for the two PV panels.



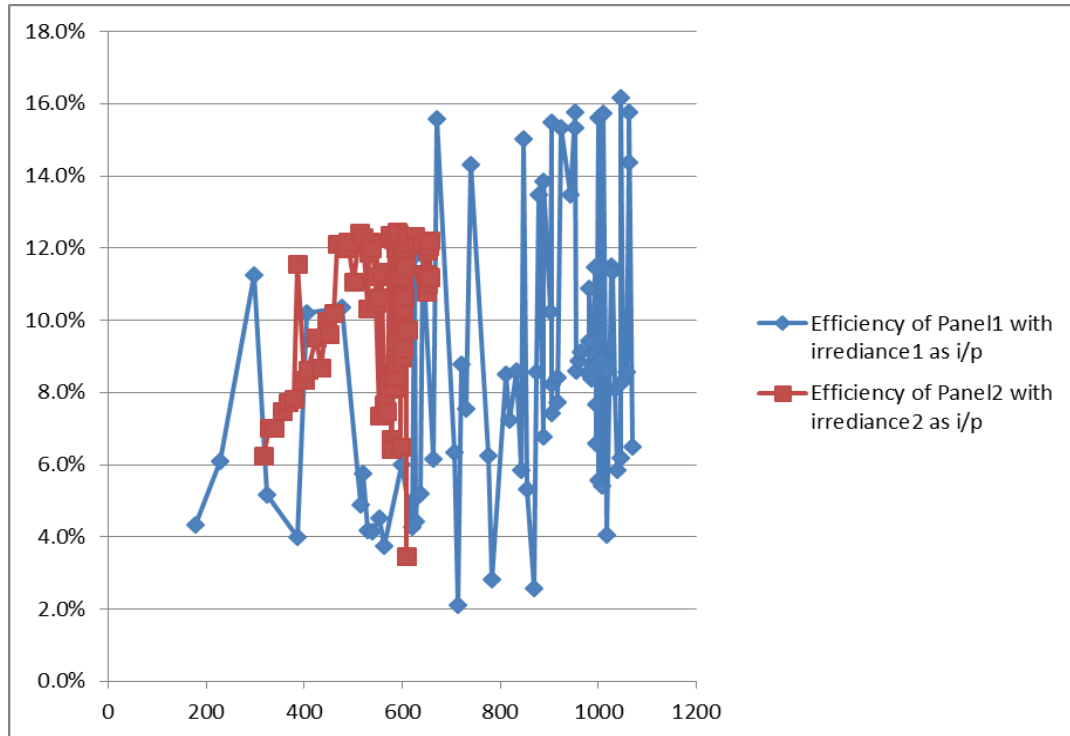


Figure 68. The various recorded efficiency of the two PV panels during the experiment.

Appendix D shows the calculated efficiency for all the runs.

### Validation

The PV panel was subjected to the founded optimum levels of treatments on the 26<sup>th</sup> of February. A sample of the data was collected from the 27<sup>th</sup> record.

Table 12. Validation sample of data. A sample of data from the 27<sup>th</sup> of February 2016 with the optimum settings of 60°, 45 ° from the south, 0 wind and 0 talc.

Date and time	Power1	Power2	Power difference	Irradiance1	Irradiance2
2/27/2016 15:45 PM	169.8W	60.5W	109.31W	1000.8W	394.25W

## **VII. CONCLUSIONS AND FUTURE WORKS**

### **Conclusions**

The four factors investigated in this research to optimize the performance of the PV panels have various impacts on the power output. In addition to these factors, other variables such as the date/time and the location of the PV panels affect the performance of the PV panels as well. To minimize the impact of the variation of the irradiance during the day, due to uncontrollable factors such as clouds and general weather conditions, this research considered the difference between the power generated by the adjustable panel (subjected to the factors) and the control panel (i.e., flat panel) as the optimization objective. An adjustable mechanical system was designed and developed for this research. Additionally, electrical and data acquisition systems were developed for this purpose as well. The research used design of experiments and response surface methodology to plan, analyze, and optimize the experiments. Minitab software was used to achieve these purposes. The final findings showed the influencing factors on the yield response. The tilt, azimuth angle (orientation), and cleanness were effective factors while wind's impact within the tested range was insignificant. The optimum findings were: 60° tilt from the horizon, 45° from the south, and panel in clean condition resulted in the maximum response (i.e., power difference between subject and control panels).

## **Future Works**

Much research can be done on PV panel performance and efficiency. Such research may include the following:

- Developing automated cleaning systems to overcome the accumulated dust problem.
- Developing smart PV panels with the capability of self-cleaning and/or self-cooling to enhance the performance.
- Developing a self-monitoring PV panel to collect the performance data.
- Enhancing the efficiency of the PV panels through studying different materials, technologies, manufacturing processes, filtering, geometry, and ads-on (e.g., built in cooling system, etc.).
- Studying the environmental effects (e.g., wind, rain, cloud, dust, humidity) on the performance of different PV panels' technologies (e.g., silicon monocrystalline, silicon polycrystalline, perovskite, etc.).
- Studying and developing optimum settings (tilt and orientation) for the PV panels for each month or permanently in designated locations.
- Studying the irradiance pattern for designated locations.
- Studying the degradation rates of PV panels at designated locations for different technologies.
- Studying the effect of the local weather conditions on the degradation rates.
- Studying the effect of pollution on both the performance and degradation rates for various PV panels' technologies.

- Collecting and recording detailed data of the PV panel performance in designated locations throughout the year.
- Creating a database for the performance of the PV panels in Texas through the cooperation with regional partners.
- Creating a cost effective, passive sun tracking system with no electrical consumption.
- Creating a cost effective, active sun tracking system with low power consumption.
- Creating a remotely-controllable, through the internet, sun tracking system for distant locations.

## **APPENDIX SECTION**

### **APPENDIX A. THE EGAUGE SOFTWARE AND CAPABILITIES**

This appendix is entirely cited and adapted from the eGauge website ("help", 2016) to describe the device settings and functions.

eGauge gathers data and can convey them to a spreadsheet programs like excel, Open office calc, or gnumeric. A friendly graphic user interface (GUI) will help to achieve that. The kind of data, time-range, and resolution of the conveyed data can be selected through this GUI. The data to be exported as a csv file can be the average values during successive time or cumulative values. Kilowatts (kW) will be the unit for the energy if exported as average values, while the unit will be kilowatt-hours (kWh) if exported as cumulative values. The time range can be specified by the user with the selection of the beginning and the ending of the time period. Another important feature eGauge provides is the time interval between data points; the default is one data point exported per day (which can be changed by the user for one data point exported per hour, minute, or second). These exported data are arranged from the newest to the oldest. To plot them the user needs to invert the time order to make the advancement of time from left to right. Such inversion can easily be done by the spreadsheet programs by using the sort function for the exported data before plotting them.

The general settings of the eGauge include: the date and time, the geographic location, the geographic region, the minimum interval for public usage data, the proxy-server hostname, and data sharing. The date and time is when record-keeping is initiated, overlooking any data chronicles before it without losing them, and later the user can

easily shift this point of time toward any direction if needed. The software gives another helpful option for the record starting point. By putting “now” as the starting date and time, the user establishes that moment as the starting point, automatically ignoring earlier data. The geographic location setting will identify the geographic location of the eGauge with a small modification to ensure the exact location will not be exposed. It includes the latitude and longitude of the site with a positive value for northern latitudes and a negative for southern latitudes, and in the same manner, a positive value will be issued to the eastern longitudes while a negative to the western longitudes. Another feature is the map, which will provide a separate window to show the map of the entered location. The geographic region shows where the eGauge is installed and guarantees regulatory compliance by controlling the frequency bands used if a home plug av interface is used. The minimum interval for public usage data setting is used to make a limitation on the data available for public users by controlling its resolution. The default of the data resolution is one minute and it can be changed to many other options that can reduce the resolution to boost security. The local and licensed users will have full-resolution data. The proxy-server hostname setting will indicate the hostname (or IP address) of the machine that is running the proxy-server. The proxy-server makes it feasible to connect to eGauge at URI <http://name.egaug.es>. Data Sharing will control the sharing of the collected data, which can be disabled or enabled, with a service provider. This sharing can also be customized to advance the collected data to a URI (unless an empty string is placed instead of it) with a particular push option and specific push interval that will define the time interval between consecutive data pushes. There are various push options and they can be used to indicate what or how data are being pushed, including calculate

totals and virtual registers, push the data with second by second granularity, compress the push data, and secure connections that demand the server has an authentication which can be confirmed as legitimate. All the above push options are separated by commas when they are listed together.

The network settings include: the hostname setting, the automatically obtain address with dynamic host configuration protocol (DHCP) setting, the IP address setting, the netmask setting, the network setting, the broadcast address setting, the gateway address setting, the name server setting, and the enable bridging setting. The hostname is a setting that will define the hostname of the eGauge, changing this name without informing the server <http://egauge.es/> will result in losing the connectivity with it. “Automatically obtain address with DHCP” is the setting that will determine whether the eGauge will manually be set with network configuration or it will do that automatically via the DHCP. If the latter option is selected then the rest of the network setting will be grayed out. The IP address setting will statically assign the eGauge an IP address (e.g., 192.168.0.99). The netmask setting will assign the IP mask address for the eGauge (e.g., 255.255.255.0). The network setting will illustrate the network IP address used by the eGauge (eg.192.168.0.0). The broadcast address setting will assign the IP broadcast address used by the eGauge (e.g., 192.168.0.255). The gateway address setting will assign the IP address of the gateway used by the eGauge (e.g., 192,168.0.1). The name server setting 1-4 will specify the IP address of the domain name system (DNS) servers which used by the eGauge. The DNS servers are used to resolve the domain-names. The eGauge typically uses a single network interface to communicate, such as a homeplug or hardware Ethernet. If we have both interfaces and the enable bridging setting is on, the

interfaces will be bridged together. The eGauge in this case will forward all the traffic between them, forming one logical network. This scenario is helpful when numerous eGauges are installed at one site, hardwiring one eGauge and the second one can connect to it using the homeplug, all the devices will be joined in the LAN. Spanning tree protocol (STP as defined by IEEE 802.1D) in this mode are enabled to detect and prevent the looping resulting from the redundancy which might over flood the LAN with the same looped packets. The manufacturer advises to design the connections carefully with no loops or use equipment that back STP.

Building automation control network (BACnet) protocol, the eGauge software contains many settings for this protocol: enable BACnet support setting, protocol to use for BACnet data link setting, BACnet device id unique to this device setting, and energy unit setting. The first setting is to enable its support which the manufacturer does not recommend selecting if the user has no knowledge of this protocol. The second setting is for the protocol to use for BACnet datalink, eGauge can communicate BACnet either through the Ethernet packets or over BACnet/IP (BIP). There are many other of datalink for the BACnet like ARCNET, MS/TP over RS-485, Point-To-Point over RS-232, and LonTalk, but the eGauge is not supporting them directly, encapsulating BACnet data inside UDP/IP packets. In our experiment the selection for this option is Ethernet since this what we use for the datalink. The third setting is for BACnet device id unique to this device, as each BACnet-capable device needs to have a unique device instance number, which can be any number between 0 and 4,194,303. And finally the energy unit setting, where the unit used for the cumulative value of energy registers will be set by this setting. The default is watt-second (Ws), while the alternative is kilowatt-hours (kWh).



Another feature the eGauge software provides is an alert service. This can be done through the alert settings and select how the eGauge will dispatch many alerts through short message service (sms) to a phone, email, or both. The recipients of such alerts can be up to four. Those alerts can be prioritized with the settings. The alerts have a delay of 30 seconds. The alerts are divided into two kinds, system defined and user defined. The first one can dispatch circumstances like a change in the eGauge configuration occurred or a connection to a remote device has been formed. User defined alerts on the other hand can be provoked by events defined by the user like a drop in solar production below a certain value.

The software of the eGauge can specify how the alert is conveyed to the desired recipient by setting the email Gateway with the hostname of mail server. The eGauge will try to send the email straightly to the destination address. The same thing can be said about the SMS which will be send to sms-gateway, yet if a firewall has been set to prevent this direct connection, the eGauge settings can include hostname of a mail server who will forward the email to the desired destination. This server can be on the same LAN, Which will take the email without authentication, or a mail server on the internet that the eGauge user has a valid account on, through the settings the username and password will be provided and then the device will use that mail server. in another word the eGauge tries to send the messages by using simple mail transfer protocol (SMTP) to the mail exchange hosts articulated by Mail exchange records (MX-records) for a given domain. If no MX records happen, then the eGauge will try to send the message to the server linked to the domain name. The setting that includes a hostname will make the eGauge convey all mail through this host. Filling the part of username for mail server in

the settings makes the eGauge convey the mail with transport layer security (TLS) encryption and the authentication through port 587 of the host, authenticating itself with the specified username and password. If no username is provided in the settings the delivery will be in plain text through port 25.

### **Alert Destinations**

It can be set to four recipients with messages of different level of priorities.

### **Message Format**

The message format is an option to choose whether to send all the pending alerts with one email (by selecting Email), the other option will send only the most recent alerts with highest priority, keeping the message size below 140 characters (by selecting short Email). The format also includes selecting mobile service provider to send the SMS through it.

### **Email address or phone number**

In this setting the email address will provided here and for SMS the phone number.

### **Minimum Alert Priority**

This setting will determine the least priority number of an alert that can start sending message to the alert destination.

### **System Alert Priorities**

Although they are predefined, they can be controlled by selecting their priority and which recipients they will deliver to. The priority is defined by assigning numbers with 0 as the minimum (will not trigger sending to anyone) and 7 as the highest.

## **User-defined Patterns**

It is comprised of many settings starting with the name of the user defined alert patterns. The name will inform the recipient of the alert about the nature of the alert condition. If this setting is kept blank then no user defined will be used in the system. The trigger condition is another setting, when they are satisfied they will initiate the alert to be sent. These conditions are consisting of three parts, left side, comparison operator, and right side. There are many types of comparison operators used by the software, less than (" $<$ "), less or equal (" $\leq$ "), equal (" $=$ "), greater or equal (" $\geq$ "), or greater (" $>$ "). They are used to compare the right hand side to the left side and if the comparison is true then the alert will be initiated. Another important setting associated with this subject is the frequency of the trigger conditions to be checked, which can be from one second to up to one year. That being said the eGauge software does an evaluation of all the alert conditions when the device is starting up, and the first minute of each hour (checking the hourly conditions), The first hour of each day (checking the daily conditions), The first hour of Sunday (checking the weekly conditions), the first hour of the first day of the month (checking the monthly conditions), the first hour or the year (checking the yearly conditions). The settings include the message to be sent to the recipient which by default shows the conditions with the right side, operator, and left side.

## **Access Control**

This part of the software settings will allow the user to control who can access the eGauge and how. It allows up to 15 users to be included and defined with a unique name, setting describes how the user may access, plus a password to secure the authentication of the user identity. The software will have a default user under the name

of owner who can alter the setting of the device when connected through the Local Area Network (LAN). That is both the user and the eGauge are having the same network name address. A new user to be easily added through the access settings. The name of the user can have letters, digits, or underscore character “\_” but it can’t be administrator as this name is reserved. Then that user can be assigned to special privileges through the settings which include:

- Viewing all the data plus altering the settings from anywhere.
- View all the data and change the settings only from the LAN.
- View all the data and the eGauge settings without the capability to change the settings.
- View limited data for a specific user.

The password for the access control settings is to be defined and set for each user, the only downside of the software password for access control setting is when the user changes the password, it will be sent via the internet to the device without any encryption. This might carry the risk of having someone intercepting this information and steal the password.

## **Date & Time**

The settings of the date and time in the software include:

Time-server (NTP) hostname(s): This setting will provide the eGauge with an IP address or hostname who will supply it with the current time. Network Time protocol (NTP) is used to provide the time. Four servers in the north-america.pool.ntp.org domain are the default to supply the time in the North American region. This is expressed by

`{0..3}.north-america.pool.ntp.org` The software can have up to eight server-names which can be done by the brace expansion. The time zone is another setting that we can add and select the one that match our location.

APPENDIX B. THE EXPERIMENT'S RUNS. THE EXPERIMENT'S RUNS AS GENERATED BY MINITAB SOFTWARE.

StdOrder	A=Tilt Angle	B= Orientation Angle	C= Wind level	D= Cleanness level
1	30	-45	1	0
2	0	-45	1	1
3	0	0	2	1
4	60	0	2	1
5	30	0	0	2
6	30	0	0	2
7	30	45	1	0
8	30	0	2	2
9	60	0	2	1
10	30	45	1	2
11	30	0	1	1
12	30	0	1	1
13	30	-45	2	1
14	60	45	1	1
15	0	0	0	1
16	0	45	1	1
17	60	0	1	2
18	0	0	1	2
19	30	0	0	0
20	0	0	0	1
21	60	0	1	0
22	60	0	2	1
23	30	45	0	1
24	30	-45	1	2
25	30	-45	0	1
26	30	-45	2	1
27	30	45	1	0
28	30	0	1	1
29	30	45	0	1
30	30	0	1	1
31	0	0	1	0
32	30	-45	1	2
33	0	-45	1	1
34	30	45	0	1
35	30	0	0	0
36	0	0	1	0
37	0	-45	1	1
38	30	45	1	2
39	60	45	1	1
40	60	0	1	2

StdOrder	A=Tilt Angle	B= Orientation Angle	C= Wind level	D= Cleanness level
41	30	-45	0	1
42	30	45	1	2
43	30	0	1	1
44	60	0	0	1
45	30	45	2	1
46	0	0	1	2
47	60	-45	1	1
48	30	-45	2	1
49	30	0	1	1
50	30	0	2	0
51	60	0	1	0
52	60	-45	1	1
53	0	45	1	1
54	30	0	1	1
55	0	0	2	1
56	30	0	2	2
57	0	0	2	1
58	30	45	2	1
59	30	-45	1	0
60	30	-45	1	2
61	30	45	2	1
62	0	0	1	0
63	30	0	2	0
64	30	0	0	2
65	60	0	1	2
66	30	0	0	0
67	0	0	0	1
68	0	0	1	2
69	60	0	0	1
70	60	0	0	1
71	60	0	1	0
72	30	0	2	2
73	30	-45	1	0
74	30	0	1	1
75	60	45	1	1
76	30	0	1	1
77	60	-45	1	1
78	0	45	1	1
79	30	0	2	0
80	30	45	1	0
81	30	-45	0	1

APPENDIX C. THE COLLECTED DATA. THE RUNS AND THE COLLECTED DATA FOR VARIOUS VARIABLES.

StdOrder	Noise factors			Irradiance		Responses				
	Panel 1 Temp	Panel 2 Temp	Amb. Temp	1	2	Power 1	Power 2	Volt. 1	Volt. 2	Power diff.
1	35.5	31.9	15.6	904	650	156	80.7	32	23.14	75.3
2	33	32	15.3	720	652	70.6	81.5	21.5	23.16	-10.9
3	30.3	31.5	15.8	888	655	67	82	21	23.2	-15
4	32.1	31.5	16.33	1064	656	170.4	82	33.3	23.2	88.4
5	35.8	32.4	16.3	1038	656	67.5	82	21.04	23	-14.5
6	37	32.8	16.3	1035	652	93.5	82	24.7	23.2	11.5
7	38	33	17.3	944	653	142	81	30.5	23.14	61
8	37.6	31.8	16.7	1070	650	77.5	81.1	22.5	23.08	-3.6
9	36	30.9	16.9	1052	647	97.5	79.4	25	22.86	18.1
10	35	32.5	17.5	1046	640	72	77	21.7	22.6	-5
11	32.5	29	18	996	631	73	75	21.8	22.25	-2
12	32.4	30	17.73	981	625	93	73	24.6	21.9	20
13	30.7	30.5	18.5	731	610	61.5	71.2	20.06	21.6	-9.7
14	31.5	30.9	18.5	990	601	100	68.8	25.5	21.3	31.2
15	32.5	28.9	19	598	600	40	68.3	16.2	21.3	-28.3
16	30	27.3	19	553	588	27.8	65.5	13.45	20.74	-37.7
17	30	27.3	19	1014	577	97	62.6	25.16	20.35	34.4
18	30.6	26.6	19.2	563	558	23.5	59.9	12.4	19.89	-36.4
19	32	28	19.8	924	554	158	58	32	19.6	100
20	33.4	27.8	19.2	529	547	24.6	58	12.86	19.5	-33.4
21	33	27	19.2	964	521	98	52	25.2	18.5	46
22	33	29.5	20	981	533	103	54.7	25.9	19	48.3
23	34.6	26	20	906	512	83	50.3	23.29	18.21	32.7
24	31.6	26.4	20	539	500	25	48.5	12.9	17.9	-23.5
25	29.4	27	20.4	520	488	33.4	47	14.7	17.6	-13.6
26	29.1	26	20.4	514	484	28	45	13.47	17.3	-17
27	30	26.3	20.4	888	467	137	43.9	29.8	16.97	93.1
28	31.43	25.9	20.1	834	459	80	41.5	22.8	16.53	38.5
29	33.3	26.5	21	873	451	83.5	40.9	23.3	16.39	42.6
30	33.8	26.3	20.5	811	445	77	38	21.9	16	39
31	31	25.6	20.5	405	433	46	37.7	17.37	15.87	8.3
32	30	26	21	386	424	17.2	36.5	10.6	15.6	-19.3
33	26	25	21.4	323	408	18.6	34	11	15	-15.4
34	27.2	24.9	20.8	819	400	66	33.4	20.8	14.7	32.6
35	29.2	24.8	21.2	740	386	118	31.7	27.6	14.38	86.3
36	30	25.6	21.5	297	378	37.3	29.6	15.5	14.11	7.7
37	32	25.3	21.3	228	366	15.5	28.6	10.2	13.77	-13.1
38	33.4	25	21.2	854	354	50.6	26.5	18	13.37	24.1
39	31.6	25	25	955	339	91.4	24.5	24.28	12.8	66.9
40	32.6	25	21.5	870	328	25	23.5	12.9	12.5	1.5



StdOrder	Panel 1 Temp	Panel 2 Temp	Amb. Temp	1	2	Power 1	Power 2	Volt. 1	Volt. 2	Power diff.
41	30.2	24.2	21.3	178	316	8.6	22	7.5	12	-13.4
42	20.6	20.1	9.2	663	582	45.5	67	17.25	21.3	-21.5
43	24.7	20	10.4	995	589	85	68	23.5	21.45	17
44	27	20.1	10.1	993	599	127	71	28.8	21.7	56
45	28	20.5	10.4	775	608	54	72	18.8	21.9	-18
46	24.7	22.6	10.8	714	569	16.8	76	10.7	22.4	-59.2
47	22.9	22.2	11.4	902	575	103	76.9	25.8	22.6	26.1
48	25.2	22.9	11.2	917	584	86	78	23.7	22.9	8
49	25.2	23	11.2	986	586	94.8	79	24.8	23	15.8
50	27.8	24	11.8	1000	590	174	80	33.6	23	94
51	28.8	24.7	11.7	1064	591	187	80.4	34.8	23.1	106.6
52	29.7	25	12.3	879	594	132	81	29	23	51
53	27	25	12.7	707	597	50	81	18.1	23.2	-31
54	27.4	25	12.4	1005	601	100	23.3	25.5	23.3	76.7
55	27.5	27.2	13.3	1002	602	96	82.7	25	23.46	13.3
56	28	27.7	13.8	1017	602	46	82.8	17.3	23.46	-36.8
57	27	24.9	13.7	638	601	36.9	83.3	15.6	23.45	-46.4
58	26.8	24	14	905	602	75	83.7	22.1	23.4	-8.7
59	27.7	25.9	14	848	610	142	83.5	30.34	23.46	58.5
60	28.5	26.6	13.9	843	609	55	83.9	19.06	23.46	-28.9
61	29	27.3	13.7	918	607	79	83.8	22.69	23.4	-4.8
62	28.2	28.3	14.5	641	608	84.4	83.3	23.39	23.38	1.1
63	28.9	29	14.4	1010	605	177	83	33.96	23.3	94
64	29.6	27.8	14.4	1009	604	61	82.8	20	23.2	-21.8
65	30	28.7	14.9	1059	602	101	81	25.6	23.2	20
66	31	29	15	624	599	82	80	23.07	23	2
67	31.3	29.4	14.7	628	597	31	81	14.3	23	-50
68	30.7	29	15.3	621	595	29.5	80.4	13.94	22.93	-50.9
69	30.1	29.5	15.2	1029	591	130	79.8	29	22.8	50.2
70	31	28.6	15.6	1027	589	131.7	79.4	29.2	22.7	52.3
71	32	29.2	15.3	1047	586	188.8	78	34.9	22.6	110.8
72	32	29.3	16.1	986	583	92	77.9	24.5	22.53	14.1
73	32.1	29.3	15.5	671	578	116.5	76.5	27.5	22.39	40
74	32.3	28.8	16	961	574	95	76	24.8	22	19
75	31	27	16.4	982	568	119	73.6	27.8	21.8	45.4
76	31	27	16.7	1000	562	62	72	20	21.7	-10
77	29.3	28.7	16.5	477	553	55	71.2	18.8	21.5	-16.2
78	27.1	29.7	17	782	546	24.7	69	12.69	21.2	-44.3
79	27.4	29.4	16.5	953	537	167.6	67	33	21	100.6
80	29.2	29.7	17.5	954	534	163	67	32.5	20.8	96
81	30.5	29.8	17	629	529	35.8	65.3	15.42	20.68	-29.5

APPENDIX D. THE EFFICIENCY CALCULATIONS. THE EFFICIENCY CALCULATED THROUGHOUT THE EXPERIMENT.

StdOrder	Efficiency of Panel1 with irradiance2 as i/p	Efficiency of Panel1 with irradiance1 as i/p	Efficiency of Panel2 with irradiance 2 as i/p	The gain in irradiance in kW/m <sup>2</sup>
1	21.52%	15.48%	11.13%	254
2	9.71%	8.79%	11.21%	68
3	9.17%	6.77%	11.23%	233
4	23.30%	14.36%	11.21%	408
5	9.23%	5.83%	11.21%	382
6	12.86%	8.10%	11.28%	383
7	19.50%	13.49%	11.12%	291
8	10.69%	6.50%	11.19%	420
9	13.52%	8.31%	11.01%	405
10	10.09%	6.17%	10.79%	406
11	10.38%	6.57%	10.66%	365
12	13.35%	8.50%	10.48%	356
13	9.04%	7.55%	10.47%	121
14	14.92%	9.06%	10.27%	389
15	5.98%	6.00%	10.21%	-2
16	4.24%	4.51%	9.99%	-35
17	15.08%	8.58%	9.73%	437
18	3.78%	3.74%	9.63%	5
19	25.58%	15.34%	9.39%	370
20	4.03%	4.17%	9.51%	-18
21	16.87%	9.12%	8.95%	443
22	17.33%	9.42%	9.20%	448
23	14.54%	8.22%	8.81%	394
24	4.48%	4.16%	8.70%	39
25	6.14%	5.76%	8.64%	32
26	5.19%	4.89%	8.34%	30
27	26.31%	13.84%	8.43%	421
28	15.63%	8.60%	8.11%	375
29	16.60%	8.58%	8.13%	422
30	15.52%	8.52%	7.66%	366
31	9.53%	10.19%	7.81%	-28
32	3.64%	4.00%	7.72%	-38
33	4.09%	5.16%	7.47%	-85
34	14.80%	7.23%	7.49%	419
35	27.42%	14.30%	7.37%	354
36	8.85%	11.26%	7.02%	-81
37	3.80%	6.10%	7.01%	-138
38	12.82%	5.31%	6.71%	500
39	24.18%	8.58%	6.48%	616
40	6.84%	2.58%	6.43%	542

StdOrder	Efficiency of Panel1 with irradiance2 as i/p	Efficiency of Panel1 with irradiance1 as i/p	Efficiency of Panel2 with irradiance 2 as i/p	The gain in irradiance in kW/m²
41	2.44%	4.33%	6.24%	-138
42	7.01%	6.15%	10.32%	81
43	12.94%	7.66%	10.35%	406
44	19.01%	11.47%	10.63%	394
45	7.97%	6.25%	10.62%	167
46	2.65%	2.11%	11.98%	145
47	16.07%	10.24%	11.99%	327
48	13.21%	8.41%	11.98%	333
49	14.51%	8.62%	12.09%	400
50	26.45%	15.61%	12.16%	410
51	28.38%	15.76%	12.20%	473
52	19.93%	13.47%	12.23%	285
53	7.51%	6.34%	12.17%	110
54	14.92%	8.92%	3.48%	404
55	14.30%	8.59%	12.32%	400
56	6.85%	4.06%	12.34%	415
57	5.51%	5.19%	12.43%	37
58	11.17%	7.43%	12.47%	303
59	20.88%	15.02%	12.28%	238
60	8.10%	5.85%	12.36%	234
61	11.67%	7.72%	12.38%	311
62	12.45%	11.81%	12.29%	33
63	26.24%	15.72%	12.30%	405
64	9.06%	5.42%	12.29%	405
65	15.05%	8.55%	12.07%	457
66	12.28%	11.79%	11.98%	25
67	4.66%	4.43%	12.17%	31
68	4.45%	4.26%	12.12%	26
69	19.73%	11.33%	12.11%	438
70	20.05%	11.50%	12.09%	438
71	28.89%	16.17%	11.94%	461
72	14.15%	8.37%	11.98%	403
73	18.08%	15.57%	11.87%	93
74	14.84%	8.87%	11.87%	387
75	18.79%	10.87%	11.62%	414
76	9.89%	5.56%	11.49%	438
77	8.92%	10.34%	11.55%	-76
78	4.06%	2.83%	11.33%	236
79	27.99%	15.77%	11.19%	416
80	27.38%	15.32%	11.25%	420
81	6.07%	5.10%	11.07%	100

## REFERENCES

- Aliexpress.com. (2016). *Buy Products Online from China Wholesalers at Aliexpress.com*. Retrieved 30 January 2016, from <http://www.aliexpress.com/item/Adjustable-300W-10-ohm-Tube-Resistors-300-Watt-Wirewound-Ceramic-Resistance-on-Sales/32341039664.html>
- Anderson, M.C. (2010) U.S. Patent No. 2010/0139735. Washington, DC: U.S. Patent and Trademark Office.
- Anthony, J. (1988). U.S. Patent No. 4,728,878. Washington, DC: U.S. Patent and Trademark Office.
- Boylestad, R. L., & Nashelsky, L. (1996). *Electronics: A Survey of Electrical Engineering Principles* (4th Ed.). Englewood Cliffs, NJ: Prentice Hall.
- Butler, D. M. (1978). U.S. Patent No 4,075,034. Washington, DC: U.S. Patent and Trademark Office.
- Cano, J. (2011). *Photovoltaic Modules: Effect of Tilt Angle on Soiling*. (Master's thesis), Engineering Technology, Arizona State University, Arizona.
- Central Electricity Regulatory Commission. (2011). Performance of Solar Power Plants in India, New Delhi, India: <http://www.cercind.gov.in>
- Chiras, D. (2011). *The homeowner's guide to renewable energy*. Gabriola Island, Canada: New Society Publishers.
- CRmagnetics Inc. (n.d.). DC Current Transducer [Brochure]. St. Louis, MO: CRmagnetics Inc.

- Daniel Sullivan. (2014, July 28). The danger of micro inverters [Web log post]. Retrieved from <http://www.sullivansolarpower.com/about/solar-power-blog/daniel-sullivan/dangers-of-micro-inverters>
- Dorobantu, L., Popescu, M. O., Popescu, C., Craciunescu, A, (2011). “The Effect of surface Impurities on Photovoltaic Panels,” International Conference on Renewable Energy and Power Quality.
- eGauge systems LLC. (2015). eGauge Model EG30xx Owner’s Manual(v1.0) [pamphlet]. Boulder, CO: eGauge Systems LLC.
- Ford, J. (2004). U.S. Patent No. 6,774,299 Washington, DC: U.S. Patent and Trademark Office.
- Goswami, Y., Kreith, F., & Kreider, F. (2000). *Principles of solar engineering* (2nd Ed.). New York, NY: Taylor & Francis Group.
- GreenRay, Inc. (2010). Sunsine 200 ac module. Retrieved from <http://www.greenraysolar.com/sites/default/files/GreenRay-SunSine200ACMod.p>
- He, G., Zhou, C., and Li, Z. (2010). “Review of Self-Cleaning Method for Solar Cell Array.” Elsevier.
- Help. (2016). Egaug7056.egaug.es. Retrieved 25 March 2016, from <http://egaug7056.egaug.es/help.html>
- Honsberg, C. & Bowden, S. (N. D.). *Degradation and Failure Modes*. Retrieved from: <http://pveducation.org/pvcdrom/modules/degradation-and-failure-modes>
- Hsieh, J. (1986). Solar energy engineering. Englewood Cliffs, N.J.: Prentice-Hall.

- Jaiganesh, K. & Duraiswamy, K, (2013). “Improving the Power Generation from Solar PV Panel Combined with Solar Thermal System for Indian Climatic Condition.” International Journal of Applied Environmental Sciences (ISSN 0973-6077). Volume, Number 6.
- Jordan, D. C., & Kurtz, S. R. (2013). Photovoltaic Degradation Rates-an Analytical Review. *Progress In Photovoltaics*, 21(1), 12-29. doi:10.1002/pip.1182
- Kaplani, E. (2012). Detection of Degradation Effects in Field-Aged c-Si Solar Cells through IR Thermography and Digital Image Processing. *International Journal Of Photoenergy*, 1-11. doi:10.1155/2012/396792
- Lam, W. (2009). Should You Spring Clean Your Solar Panels. Google official blog. Retrieved from <https://googleblog.blogspot.com/2009/07/should-you-spring-clean-your-solar.html>
- Livingonsolarpower. (2013, June 10). Solar PV Power Plants: Major Causes of Performance Degradation [Blog Post]. Retrieved From: <https://livingonsolarpower.wordpress.com/2013/06/10/solar-pv-power-plants-major-causes-of-performance-degradation/>
- Mani, M. & Pillai, R. (2010). Impact of Dust on Solar Photovoltaic (PV) Performance: Research Status, Challenges and Recommendations. *Elsevier*.
- Marten, K., Rau, U. (2007). Renewable energy. M. Kaltschmitt, W. Streicher, & A. Wiese(Ed.). Heidelberg, Germany: Springer.

- Mazumder, M., Horenstein, M., Stark, J., Girouard, P., Sumner, R., Henderson, B., Sadler, O., Hidetaka, I.Z, A., & Sharma, R. (2011). "Characterization of Electrodynamic Screen Performance for Dust Removal from Solar Panels and Solar Hydrogen Generators." IEEE.
- Mekhilef, S., Saidur, R., Kamalisarvestani, M, (2012). "Effect of Dust, Humidity and Air Velocity on Efficiency of Photovoltaic Cells." Elsevier.
- Moharram, K. A., Abd-Elhady, M. S., Kandil, H. A., and Elsherif, H. (2013). "Influence of Cleaning Using Water and Surfactants on the Performance of Photovoltaic Panels." Elsevier.
- Mondol, J. D., Yohanis, Y. G., Norton, Y. B. (2006). "The Impact of Array Inclination and Orientation on the Performance of a Grid-Connected Photovoltaic System." Elsevier.
- Montgomery, D. (1997). Design and analysis of experiments. New York: Wiley.
- Myers, R. H., & Montgomery, D. C. (2002). *Response surface methodology: process and product optimization using designed experiments*. New York: J. Wiley, c2002.
- National Renewable Energy Laboratory (2015), Efficiency chart [online image]. Retrieved from [www. Nrel.gov/ncpv/images/efficiency\\_chart.jpg](http://www.nrel.gov/ncpv/images/efficiency_chart.jpg)
- Neitzel, F. (2016). Solar Tracking, Solar Tracking Systems, Solar Trackers | We Catch the Sun. Solar-tracking.com. Retrieved 20 March 2016, from <http://www.solar-tracking.com/>
- Odeh, S., & Behnia, M, (2009). "Improving Photovoltaic Module Efficiency Using Water Cooling." Tylor & Francis Group.

Oliver, J. A. (2013). U.S. Patent No. 8,492,929 B2. Washington, DC: U.S. Patent and Trademark Office.

Prasad, R. D., (2011). *Handbook of renewable energy technology*. A. Zobaa, & R. C. Bansal (Ed.). Toh Tuck Link, Singapore: World scientific publishing Co. Pte. Ltd.

Rabinowitz, M. (2005). U.S. Patent No. 2005/0034750. Washington, DC: U.S. Patent and Trademark Office.

Rajput, D., & Sudhakar, K. (2013). “Effect of Dust on the Performance of Solar PV Panel.” International Conference on Global Scenario in Environment and Energy.

Schutten, H. P., Benjamin, J. A., & Lade, R. W. (1986). U.S. Patent No. 4,577,052 Washington, DC: U.S. Patent and Trademark Office.

Shepherd, W., & Shepherd, D. W. (2014). *Energy studies* (3rd Ed.). London, England: Imperial College Press.

Skoplaki, E. & Palyvos, J. A, (2008). “On the Temperature Dependence of Photovoltaic Module Electrical Performance: A review of Efficiency/Power Correlations.” Elsevier.

SMA America, LLC. (2011). *Ambient Temperature Sensor Tempsensor-Ambient Installation Guide* [Pamphlet]. Denver, CO: SMA America, LLC.

SMA America, LLC. (2011). *System Monitoring Sunny Senesorbox Installation Guide* [Pamphlet]. Denver, CO: SMA America, LLC.

SMA Solar Technology AG. (2009). *System Monitoring PT100m-NR Installation Guide* [Pamphlet]. Niestetal, Germany: SMA Solar Technology AG.



Smee, A. (1849). Elements of electro-biology, or, The voltaic mechanism of man.

London: Longman, Brown, Green & Longmans.

Solar Systems USA Online Solar Panels. (2016). *Pallet of Eopllly 190 Watt Mono Solar Panel*. Retrieved 30 January 2016, from <http://www.solarsystems-usa.net/solarpanels/eopllly/ep125m-72-190/>

Sørensen, B. (2011). Renewable energy. Burlington, MA: Academic Press.

Sulaiman, S. A., Singh, A. K., Mokhtar, M. M. M., Mohammed, A. B, (2014). Influence of Dirt Accumulation on Performance of PV Panels. *Elsevier*.

Surles, W., Baum, J., Watrous, A., Johnson, S., Horanyi, E., Zarske, M. S, (2009).

“Photovoltaic Efficiency Lesson 2 the Temperature Effect”. Regents of the University of Colorado. Retrieved from:

[https://www.teachengineering.org/collection/cub\\_/lessons/cub\\_pveff/Attachments/cub\\_pveff\\_lesson02\\_fundamentalsarticle\\_v6\\_tedl\\_dwc.pdf](https://www.teachengineering.org/collection/cub_/lessons/cub_pveff/Attachments/cub_pveff_lesson02_fundamentalsarticle_v6_tedl_dwc.pdf)

Tester, J., Drake, E., Driscoll, M., Golay, M., & Peters, W. (2012). *Sustainable energy: Choosing among options* (2nd Ed.). Cambridge, MA: The MIT Press.

The nobel prize, n.d. Retrieved from

[http://www.nobelprize.org/nobel\\_prizes/physics/laureates/1921/](http://www.nobelprize.org/nobel_prizes/physics/laureates/1921/)

Ulrich, K., & Eppinger, S. (2012). Product design and development. New York: McGraw-Hill/Irwin.

What Is A Response Surface Design? - Minitab. Support.minitab.com. N.p., 2016. Web. 21 Mar. 2016.

Zorrilla-Casanova, J., Piliouline, M., Carretero, J., Bernoaola, P., Carpena, P., Mora-Lopez, L. & Sidrach-de-Cardona, M. (2011). "Analysis of Dust Losses in Photovoltaic Modules." World Renewable Energy Congre